Aus dem Institut Max-Delbrück - Centrum für Molekulare Medizin

DISSERTATION

Calcium signalling in the nervous system

zur Erlangung des akademischen Grades Doctor of Philosophy (PhD)

vorgelegt der Medizinischen Fakultät Charité - Universitätsmedizin Berlin

von

Laura Maria Korvers M.Sc., B.ASc.

aus Halsteren, die Niederlande

Datum der Promotion: 22.09.2017

”Gedruckt mit Unterstützung des Deutschen Akademischen Austauschdienstes”

Contents

List of Figures

List of abbreviations

AMPA α - amino - 3 - hydroxy - 5 - methyl - 4 - isoxazolepropionate

ATP adenosine 5' - triphosphate

BDNF brain derived neurotrophic factor

Ca^{2+} calcium

cADPR cyclic adenosine diphosphate ribose

cAMP cyclic - adenosine monophosphate

CBX carbenoxolone

CNS central nervous system

CNTF ciliary neurotrophic factor

CPA cyclopiazonic acid

DMEM Dulbecco's Modified Eagle's Medium

ER endoplasmic reticulum

FCS fetal calf serum

GAM glioma - associated macrophages/ microglia

GDNF glial cell derived neurotrophic factor

GRP78 glucose regulated protein 78

hGAM human glioma - associated macrophages/ microglia

IP_3 inositol 1,4,5-trisphosphate

IP_3R inositol 1,4,5-trisphosphate receptor

LGIC ligand gated calcium (Ca^{2+}) channel

LPS lipopolysaccharide

MACS magnetic activated cell sorting

MCU mitochondrial Ca^{2+} uniporter

mGAM mouse glioma - associated macrophages/ microglia

mRNA messenger ribonucleic acid

MRS2578 *N,N"* - 1,4 - Butanediyl *bis* [*N'* - (3 - isothiocyanatophenyl)] thiourea

NCLX mitochondrial Na^{+}/Ca^{2+} exchanger

NGF nerve growth factor

NMDA N - methyl - D aspartate

NMDAR N - methyl - D aspartate (NMDA) receptor

NT - 3 neurotrophin - 3

NTPDase1 ectonucleoside triphosphate diphophohydrolase - 1

P2 purinergic receptor

P2X ionotropic purinergic receptor

P2Y metabotropic purinergic receptor

PLC phospholipase C

PPADS pyridoxalphosvphate - 6 - azophenyl - 2', 4' - disulfonic acid

PSG penicillin, streptomycin and glutamine

PTP permeability transition pore

RB2 reactive blue 2

RNA ribonucleic acid

RyR ryanodine receptor

SERCA sarco/ endoplasmic reticulum (ER) Ca^{2+}-ATPase

STIM stromal interaction protein

Tg thapsigargin

U73122 1-[6-[[17β-3-Methoxyestra-1, 3, 5(10)-trien-17-yl] amino]-hexyl]-1H-pyrrole-2, 5 - dione

VDAC voltage - dependent anion channel

VEGF vascular endothelial growth factor

Abstract

Calcium (Ca^{2+}) is a main secondary messenger in nearly all eukaryotic cells, including those belonging to the central and peripheral nerve system. Free intracellular Ca^{2+} ($[Ca^{2+}]_i$) in resting cells is maintained at low concentrations (submicromolar range). In contrast, the Ca^{2+} concentration in the extracellular space and the endoplasmic lumen exceeds the 10^3 - 10^6 range. This results in a cytosolic - directed Ca^{2+} flow whenever a Ca^{2+} permeable ion channel opens on the plasma or endoplasmic membrane. These Ca^{2+} flows are often triggered by extracellular ligands like neurotropic factors (brain derived neurotrophic factor (BDNF), glial cell derived neurotrophic factor (GDNF)), neurotransmitters (glutamate, NMDA) or even adenosine 5' - triphosphate (ATP). In some cases, a Ca^{2+} elevation occurs without apparent stimulation and are therefore denoted as 'spontaneous' Ca^{2+} elevations.

My doctoral work is focused on the regulation of cytosolic Ca^{2+} in cells belonging to the nerve system, with a particular interest in microglia, the immune cells of the nerve system. Like all other cells, microglia cells possess many receptors and Ca^{2+} channels in the plasma membrane, including receptors for classical neurotransmitters. Experiments in living animals revealed that microglia can display spontaneous cytosolic Ca^{2+} elevations. It was, however, unclear if these elevations were triggered by released neurotransmitters, extracellular ligands, intracellular or autocrine signalling. Therefore I performed Ca^{2+} imaging experiments with cultured microglia and detected spontaneous Ca^{2+} elevations in 50% of the isolated microglia cells in absence of neurons and other glial cells. Sequential experiments indicated that these elevations are regulated via phospholipase C (PLC), inositol 1,4,5-trisphosphate (IP_3) and inositol 1,4,5-trisphosphate receptor (IP_3R) on the endoplasmic membrane. Purinergic signalling was excluded as autocrine trigger of these events. In a second study, I showed that cultivated microglia lack functional NMDA receptors on the plasma membrane. In contrast to the *in situ* patch clamp experiments of S. Wendt, where NMDA triggered a plasma membrane current, a Ca^{2+} elevation after NMDA application remained absent *in vitro*.

In the peripheral system, increased expression of neurotropic factors (ciliary neurotrophic factor (CNTF), BDNF, GDNF, vascular endothelial growth factor (VEGF), neurotrophin - 3 (NT - 3) and nerve growth factor (NGF)) could lead to an increased internal Ca^{2+} concentration due to the continuous stimulation of the PLC dependent signalling

pathway(s). I investigated if long - term elevated Ca^{2+} concentration (20 weeks) could change proliferation and regeneration of nerve cells after damage. However, neurotropic factor overexpression did not improve motor or sensory recovery after sciatic nerve injury in rats.

Abstrakt

Calcium (Ca^{2+}) fungiert als wichtiger sekundärer Botenstoff in nahezu allen eucaryontischen Zelltypen inclusive Zellen des Nervensystems. Die freie, intracelluläre Ca^{2+} - Konzentration ($[Ca^{2+}]_i$) ruhender Zellen ist für gewöhnlich sehr niedrig (submikromolaren Bereich). Im Gegensatz dazu ist die extrazelluläre Ca^{2+} - Konzentration und die im Lumen des ER 10^3 bis 10^6 - fach höher, was dazu führt, dass es zu einem Ca^{2+} - Einstrom ins Cytosol kommt, wannimmer sich Ca^{2+} - permeable Ionenkanäle in der Plasmamembran oder der Membran des ER öffnen. Cytosolische Ca^{2+} - Erhöhungen können von extrazellulären Liganden, wie etwa neurotropen Faktoren (z.B. BDNF, GDNF) und Neurotransmittern (Glutamat, NMDA) oder auch ATP hervorgerufen werden. In einigen Zelltypen treten jedoch auch transiente Erhöhungen von $[Ca^{2+}]_i$ ohne offensichtliches Vorhandensein extracellulärer Liganden auf und werden deshalb als 'spontan' bezeichnet.

Ich habe mich in meiner Doktorarbeit mit der Regulation von cytosolischen Ca^{2+} in Zellen des Nervensystems beschäftigt. Insbesondere habe ich mich Mikroglia gewidmet, den Immunzellen des Nervensystems. Mikroglia besitzen wie alle Zellen viele Rezeptoren und Ca^{2+} Kanäle in der Plasmamembran - und exprimieren auch Rezeptoren für klassische Neurotransmitter. Aus Studien an lebenden Mäusen war bereits bekannt, dass Mikroglia spontane cytosolische Ca^{2+} - Erhöhungen aufweisen. Nicht klar war jedoch, ob diese Ca^{2+} - Erhöhungen durch freigesetzte Neurotransmitter oder andere extrazelluläre Liganden hervorgerufen werden oder durch intrazelluläres oder autokrines Signalling von Microglia selbst. Daher führte ich Ca^{2+} - Imaging - Experimente an kultivierten Microglia durch, und auch hier - in Abwesenheit von Neuronen und anderen Gliazellen - zeigten 50% dieser isolierten Microglia spontane Ca^{2+} - Erhöhungen. In Folgeexperimenten konnte ich zeigen, dass diese Erhöhungen über PLC, IP_3 und IP_3R in der ER-Membran reguliert werden. Purinerges Signalling als autokrinen Trigger dieser spontanen Ca^{2+} - Erhebungen konnten hingegen ausgeschlossen werden. In einer weiteren Studie konnte ich zeigen, dass kultivierte Microglia keine funktionellen NMDA - Rezeptoren in der Plasmamembran exprimieren. Im Gegensatz zu parallelen Patch - Clamp - Experimenten von S.Wendt, in denen NMDA Ströme über die Plasmamembran evozierte, fand ich *in vitro* keinerlei Erhöhung des $[Ca^{2+}]_i$ nach Applikation von NMDA.

In peripheren Neuronen kann eine Exposition von neurotropen Faktoren (CNTF, BDNF, GDNF, VEGF, NT - 3 and NGF) Erhöhungen des $[Ca^{2+}]_i$ durch Stimulation von PLC-

abhängigen Signalwegen verursachen. Ich habe untersucht, ob sich dies möglicherweise auf die Proliferation und die Regeneration von Nervenzellen nach einer Schädigung auswirkt. Eine langfristige Überexpression von neurotropen Faktoren (20 Wochen) verbesserte jedoch nicht die motorische oder sensorische Erholung nach Ischiasnervenschäden bei Ratten.

1 Summary

1.1 Introduction

Ca^{2+} is a widely used second messenger. Small changes in Ca^{2+} concentrations can be easily detected and regulates messenger ribonucleic acid (mRNA) and protein processing. Consequently, many channels and receptors are inserted into the plasma membrane and other organelles to manipulate the intracellular Ca^{2+} concentration.

Plasma membrane bound channels and receptors Voltage gated Ca^{2+} channels can be divided in 3 main groups (Ca_v1, Ca_v2 and Ca_v3). Each voltage gated Ca^{2+} channel consists of multiple subunits, allowing participation in various cellular processes. These channels are known to regulate functions as neurotransmitter release, synaptic vesicle fusion, neuronal firing patterns and excitability (Zamponi et al., 2015).

Ligand gated Ca^{2+} channels (LGICs) family comprises 3 super families (cys - loop, ionotropic glutamate and ATP - gated channels (Barry and Lynch, 2005)). Upon agonist binding, the channel transforms to its open state and ions can pass. The receptor returns to its ground closed state when the ligand dissociates. Selectivity of the channel for Na^+, K^+, Ca^{2+} and other ions are determined by subunit composition (Barry and Lynch, 2005; Burnstock and Verkhratsky, 2012).

Receptor operated Ca^{2+} channels are classified into three different groups (A - C) based on their ligands. These receptors couple with heterotrimeric G - proteins, which are released upon ligand binding. Depending on the G - protein subtypes, Ca^{2+} can be released from the ER via PLC-β - IP_3R signalling and other ion channels via cyclic - adenosine monophosphate (cAMP) (Bräuner-Osborne et al., 2007; Reece et al., 2010).

Tyrosine kinase receptors belong to the family of enzyme linked cell surface receptors. Ligand binding causes a conformational change in the receptor and the transfer of a phosphate group along specific tyrosine side chains. This results - amongst others - in the activation of PLC - γ and Ca^{2+} release from the ER via IP_3R signalling (Alberts et al., 2002).

Store operated Ca^{2+} channels are responsible for refilling the internal Ca^{2+} stores. When the Ca^{2+} concentration in the ER is low, stromal interaction protein (STIM) connects the ER with Orai in the plasma membrane, forming a Ca^{2+} channel to refill the ER (Dupont

et al., 2011).

Intracellular Ca^{2+} signalling The ER and mitochondria are the two main and best studied intracellular Ca^{2+} stores. The ER is an extensive network of membranes and consists of tubules and cisternae which is continuous with the nuclear envelope. The mitochondria are semi - autonomous organelles within cells responsible for energy production (Reece et al., 2010).

Sarco/ ER Ca^{2+}-ATPase (SERCA) transports Ca^{2+} from the cytosol into the ER at the expense of ATP (Periasamy and Kalyanasundaram, 2007). Ca^{2+} is sequestered in the ER lumen by proteins such as calreticulin ($\sim$ 50%) and glucose regulated protein 78 (GRP78) ($\sim$ 25%) (Prins and Michalak, 2011). Ca^{2+} can be released from the ER via IP_3R and ryanodine receptor (RyR). IP_3Rs are activated upon IP_3 production by PLC - β and/ or γ. IP_3Rs are reported to cause Ca^{2+} oscillations in non - cardiac cells, such as the rat Suprachiasmatic nucleus and *Aplysia* neurons (reviewed by Ju et al. (2012)). These oscillations probably depend on the Ca^{2+} load of the ER and the presence of ATP (Thrower et al., 2000). RyRs can be activated via voltage gated Ca^{2+} in the skeletal and cardiac muscle. The activation mechanism in non - excitable cells was not clear for a very long period, but recent studies in sea urchin eggs, brain, pancreatic β and acinar cells suggest that cyclic adenosine diphosphate ribose (cADPR) can activate RyR in these models (Lanner et al., 2010).

Ca^{2+} enters the mitochondria through voltage - dependent anion channels (VDACs) on the outer membrane and mitochondrial Ca^{2+} uniporter (MCU) in the inner membrane under the pressure of the mitochondrial membrane potential (Ben-Hail et al., 2014; Brookes et al., 2004; De Stefani et al., 2015; Rizzuto et al., 2009). Ca^{2+} is sequestered in the matrix by precipitating the Ca^{2+} as calciumphosphate and highly depends on an adenine free matrix, Ca^{2+} concentration and pH (Graier et al., 2007). Surprisingly, Ca^{2+} can be quickly released from the mitochondria via mitochondrial Na^+/Ca^{2+} exchanger (NCLX) and the permeability transition pore (PTP) (Rizzuto et al., 2009), suggesting that not all Ca^{2+} is precipitated.

Ca^{2+} signalling in microglia Microglia were discovered and extensively described by Pio Del Rio Hortega (1919). In the beginning of microglia research it was believed that the

microglia under physiological conditions wait in their ramified appearance until a pathological event would occur. Therefore investigators used to term these microglia 'resting' microglia (Kettenmann et al., 2011; Ransom and Kettenmann, 2012). Recent experiments revealed that microglia monitor the central nervous system and phagocytose apoptotic newborn neurons in the adult sub granular zone (Sierra et al., 2010).

Ca^{2+} signalling in microglia is regulated via a wide selection of membrane bound Ca^{2+} channels that directly gate the entrance of extracellular Ca^{2+} into the cytosol. Furthermore, microglia also have a battery of metabotropic receptors that produce IP_3 after receptor stimulation, leading to Ca^{2+} release from the intracellular Ca^{2+} stores. A selection of these receptors are activated by neurotransmitters, such as α - amino - 3 - hydroxy - 5 - methyl - 4 - isoxazolepropionate (AMPA) or purines and pyrimidines (reviewed in (Kettenmann et al., 2011; Pocock and Kettenmann, 2007; Sharma and Ping, 2014)). The functional expression of some neurotransmitter receptors by microglia are still under debate: primary cultured neonatal microglia seem to express functional NMDA receptor (NMDAR) (Kaindl et al., 2012; Murugan et al., 2011) whereas *in situ* expression could not be confirmed (Dissing-Olesen et al., 2014; Eyo et al., 2014).

Furthermore, about 22% of the microglia display spontaneous Ca^{2+} transients *in vivo*, which do not coincide with (spontaneous) astrocytic Ca^{2+} waves or (strong) neuronal activation with bicuculine (Eichhoff et al., 2011). Spontaneous activity in microglia seems to be age depended, however, as the proportion of active cells is doubled in adult compared to juvenile mice. Furthermore, the frequency of spontaneous Ca^{2+} events and the proportion of cells displaying spontaneous events is increased under pathological conditions (Brawek et al., 2014; Pozner et al., 2015). Taken together, this data suggest that spontaneous Ca^{2+} transients in microglia could play a role in maintaining cellular homeostasis.

Ca^{2+} signalling in neurons Ca^{2+} regulates neuronal function directly and indirectly for short or long periods. Ca^{2+} can immediately alter the membrane potential and consequently the properties of the voltage gated channels, regulating neuronal excitability. Other receptors use Ca^{2+} as a ligand and regulate properties of secondary channels via G - protein signalling. Ca^{2+} entry via the voltage gated calcium channels trigger vesicle release at the pre - and post - synaptic terminal of axons and dendrites (Jones and Smith, 2016).

Ca^{2+} can alter gene expression and thus regulate complex biological responses over longer periods of time. Neurotropic factors, i.a. NGF, BDNF or GDNF, trigger dimerization of tyrosine kinase receptors and consequently PLC - γ and other signalling pathways. Ca^{2+} released via this mechanism modify gene expression and coordination of cellular functions such as proliferation, differentiation and cell survival (Segal et al., 1996), but also directed neurite outgrowth after neuronal damage (Brushart, 2011).

Ca^{2+} signalling in other brain cells Astrocytes are responsible for providing the neurons with various nutrients. In order to regulate and maintain their function, astrocytes express LGIC, receptor operated Ca^{2+} channels and store operated Ca^{2+} channels. Furthermore, mature astrocytes can potentially express voltage gated Ca^{2+} channels after being exposed to some stimuli. Astroglial Ca^{2+} signals can remain localized within a sub-cellular region to regulate exocytosis or migrate within a single cell by inducing Ca^{2+} release from the ER. Ca^{2+} signals that travel to neighbouring cells are extracellularly propagated by either ATP or glutamate release or intra-cellularly by migration of IP_3 through gap junctions, triggering Ca^{2+} release from the ER in neighbouring cells (Ransom and Kettenmann, 2012).

Oligodendrocytes in the central nervous system and Schwann cells in the peripheral nervous system myelinate axons to propagate neuronal signalling. Immature oligodendrocytes express voltage gated calcium channels at the process tips, probably to identify active axons to initiate myelination (Ransom and Kettenmann, 2012). Prolonged sciatic nerve stimulation triggers Ca^{2+} release from the RyR sensitive stores and propagates extracellular Ca^{2+} entry in neighbouring Schwann cells. Furthermore, electrical stimulation of cultured dorsal root ganglion neurons caused and activity dependent Ca^{2+} increase in co - cultured Schwann cells (Rousse and Robitaille, 2006).

1.2 Methodology

1.2.1 Project 1: Ca^{2+} signalling in microglia.

Brains were extracted from neonatal (0 - 3 days old) or adult (8 - 12 week old) mice and placed on ice with HBSS after removal of the meninges, cerebellum and olfactory bulb for adult animals. Dissected brains were washed before adding trypsin, DNAse in PBS, supplemented with penicillin, streptomycin and glutamine (PSG) for adult animals. The reaction was blocked by adding Dulbecco's Modified Eagle's Medium (DMEM) containing fetal calf serum (FCS). Cells were further mechanically dissociated. The supernatant was discarded and the neonatal pellet re-suspended in DMEM and plated in poly - L - Lysine coated flasks. After 24 - 48 h of incubation, the cultures were washed and allowed to grow until confluent in DMEM. Medium was replaced by DMEM with 33% L929 conditioned medium. After 2 days, cells were harvested by shaking and plated onto coverslips. This procedure could be repeated for 2 times with 2 days interval. The adult pellet was seeded on a chlodronate-treated pre-culture and incubated. After 3 days, the cultures were washed with PBS and incubated with DMEM containing FCS and PSG. After 1 week, the medium was replaced by DMEM with 50% L929 conditioned medium. 1 week later, the cells were harvested and plated onto coverslips. This procedure could be repeated for 2 times with 7 days interval.

During life cell Ca^{2+} imaging, cells were kept in standard HEPES buffer (pH 7.4). Cells were incubated with Fluo4-AM® in standard buffer for 40 min at room temperature. Prior to the recordings, cells were washed for 10 - 15 min in standard buffer. Fluorescence signals were recorded at excitation and emission wavelengths of 488 nm and 510 nm, respectively. During recording, cells were superfused with standard buffer using a peristaltic pump. 1 mM ATP was applied for 30 sec at the end of each recording to determine the viability of the cells. Pictures were taken with a frequency of 2 frames/s and an exposure time of 50 ms using a 20x water immersion objective.

Videos were analysed using ImageJ 1.48g and further analysed with a custom made algorithm in Igor Pro 6.34A (WaveMetrics Inc. Oregon, USA) All data are given as mean $\pm$ S.E.M. Significance was tested by one-way ANOVA and post - hoc Tukey tests using Igor Pro unless stated otherwise. Significance is given by: n.s., $p > 0.05$; *, $p < 0.05$; **, $p < 0.01$; ***, $p < 0.001$.

Project 1a: Spontaneous Ca^{2+} elevations in microglia In addition to the neonatal and the adult cultured microglia, mouse glioma - associated macrophages/ microglia (GAM) were analysed. To obtain the mouse GAM, GL261-implanted mice were sacrificed 20 days post-injection, tumour-bearing and control mice were euthanized and perfused using an ice-cold PBS solution. For naïve mouse brains, the olfactory bulbs and the cerebellum were cut by a scalpel and discarded. The rest of the tissue was used for dissociation. In tumour-bearing mouse brains, only the visible tumour area around the injection site was used. Microglia were freshly isolated and purified for Ca^{2+} imaging using magnetic activated cell sorting (MACS). Microglia were isolated from cell suspensions using magnetic CD11b micro-beads™, according to the manufacturer's instructions. The tumours were dissociated using the Miltenyi Biotec Neural Tissue Dissociation Kit (Trypsin), as previously described by Nikodemova and Watters (2012). To obtain human GAM, resected human glioma were freshly isolated and purified for Ca^{2+} imaging using MACS. The human glioma tissue was manually dissociated using the Miltenyi Biotec Neural Tissue Dissociation Kit (Trypsin), according to the manufacturer's instructions.

Ribonucleic acid (RNA) was isolated using the NucleoSpin RNA kit according to the manufactures instructions.

During life cell imaging, cells were exposed to the following substances depending on the experiment for 15 min: Ca^{2+} - free buffer supplemented with EGTA, thapsigargin (Tg), cyclopiazonic acid (CPA), caffeine, 1-[6-[[17β-3-Methoxyestra-1, 3, 5(10)-trien-17-yl] amino]-hexyl]-1H-pyrrole-2, 5 - dione (U73122), ryanodine, apyrase, carbenoxolone (CBX), reactive blue 2 (RB2), pyridoxalphosvphate - 6 - azophenyl - 2', 4' - disulfonic acid (PPADS), suramin and *N,N"* - 1,4 - Butanediyl *bis* [*N'* - (3 - isothiocyanatophenyl)] thiourea (MRS2578). 12.5 min was used for analysis to exclude the wash - in/ - out phase. Cells were pre-treated with lipopolysaccharide (LPS) for 12 or 36 h prior to imaging or 12 h with bafilomycin were stated.

Project 1b: NMDA evoked Ca^{2+} elevations in microglia To test adult cultured microglia response to 100 μM NMDA, microglia were exposed to NMDA for 1 min during recording. Cells displaying spontaneous Ca^{2+} elevations, were excluded from analysis to prevent possible false - positive results.

1.2.2 Project 2: Functional recovery after prolonged neurotropic factor expression

A total of 64 young adult female Wistar rats (200-225 gram) were used. Rats were followed for a total of 20 weeks after surgery in order to assess functional recovery after sciatic nerve transection. Experiments were carried out double blinded.

10 mm of the left sciatic nerve was removed for viral infection. The tibial fascicle was injected *ex-vivo* with lentiviral vector solution (PBS, sGFP, NGF, BDNF, NT - 3, GDNF, CNTF and VEGF). Each treatment group contained 8 animals. The injected graft was placed back between the nerve stumps. Animals were allowed to recover for 14 days before being subjected to functional recovery tests.

Nerve conductance was measured from the dorsal feet muscle (innervated by the Peroneal nerve) and plantar side of the foot (innervated by the Tibial nerve). A supra-maximal stimulus was given just posterior of the lateral malleolus, using bipolar electrodes. Amplitude of the compound muscle action potential (CMAP) was recorded from the lesioned and contra-lateral side for all rats before surgery and weekly after the recovery phase for a total duration of 20 weeks.

Sensory recovery was followed with the Hargreaves and foot - flick test. For the Hargreaves test, animals were habituated for 5 min. After this period, a radiant heat source was placed directly under the feet, in front of the calcaneus. Animals were exposed maximal 20 sec to the heat stimulus to prevent tissue damage. Withdrawal time was measured 3 times in each session ipsi-lateral and contra-lateral to the injury site. Hargreaves testing was preformed every week over of 20 weeks a day prior to electro-physiology. For the foot - flick test, animals were tested at 2 week intervals between 14 weeks and 20 weeks after nerve transection. The minimal current (up to 0.5 mA to prevent tissue damage) applied to the lateral area of the foot sole needed to elicit a response was noted.

Motor recovery was assessed using motion tracking. The animals walked up to 5 times in front of a camera with markings on the proxima tibia, lateral malleolus, calcaneus and the fifth metatarsal vein. The angles of the leg of 4 essential stages of rodent locomotion were analysed: initial contact, mid stance, toe off and mid swing.

The results obtained from electro-physiology, Hargreaves test, foot - flick and motion analysis were analysed with a 2-way repeated measure ANOVA followed by a Bonferroni post hoc test using Graph Pad Prism 5.

1.3 Results

1.3.1 Project 1: Ca^{2+} signalling in microglia.

Project 1a: Spontaneous Ca^{2+} elevations in microglia First we characterized the spontaneous Ca^{2+} transients in various microglia model systems. For this we investigated freshly isolated adult (P60 - P70, 5 animals), primary cultured adult (P60 - P70, 3 independent preparations) and primary cultured microglia (18 culture preparations). The proportion of microglia displaying spontaneous activity was significantly reduced in freshly isolated adult microglia (14.4 $\pm$ 5.1%, n = 228 cells, 12 coverslips) compared to primary cultured adult (41.8 $\pm$ 7.3%, n = 221 cells, 15 coverslips, p = 0.004) and neonatal microglia (49.6 $\pm$ 2.5 %, n = 4205 cells, 89 coverslips, p = 3.6 * 10^{-6}). The frequency of spontaneous events was reduced in adult cultured (1.9 $\pm$ 0.5 events/cell * h) and freshly isolated (2.5 $\pm$ 0.4 events/cell * h) microglia compared to neonatal cultured microglia (7.8 $\pm$ 0.7 events/cell * h, p = 0.004 and p = 0.004 respectively). There was no difference between freshly isolated and cultured adult microglia (p >0.05, figure 1A - D). Primary cultured neonatal microglia were used to further identify the underlying mechanism.

Extracellular Ca^{2+} modulates the spontaneous Ca^{2+} transients Since microglia possess a large number of plasma membrane bound Ca^{2+} channels (reviewed by Kettenmann et al. (2011)), we sought to further identify their role in the generation of spontaneous Ca^{2+} transients. Three different paradigms were tested: (I) omitting Ca^{2+} from the extracellular buffer and supplementing it with EGTA (4 culture preparations), (II) unspecific blockage of membrane bound Ca^{2+} channels using ruthenium red (2 culture preparations) and (IV) Ca^{2+} entry via ionotropic purinergic receptor (P2X) with PPADS (1 culture preparation). The proportion of microglia displaying spontaneous Ca^{2+} transients was reduced under Ca^{2+} free conditions (23.5 $\pm$ 4.2%, n = 1003 cells, 25 coverslips, p = 0.0020) and increased during PPADS application (64.3 $\pm$ 5.6 %, n = 464 cells, 11 coverslips, p = 0.0120) compared to control. Ruthenium red had no effect on the spontaneous events (p >0.05). Surprisingly, PPADS increased the frequency of events (25.3 $\pm$ 3.65 events/cell * h, n = 464 cells, 11 coverslips, p <1.0 * 10^{-7}) compared to control (7.95 $\pm$ 0.62 events/cell * h). Thus, Ca^{2+} entry via the plasma membrane bound Ca^{2+} channels can modulate the spontaneous Ca^{2+} transients, but are not the main Ca^{2+} source. This suggests that internal Ca^{2+} stores play a main role in the generation of these events.

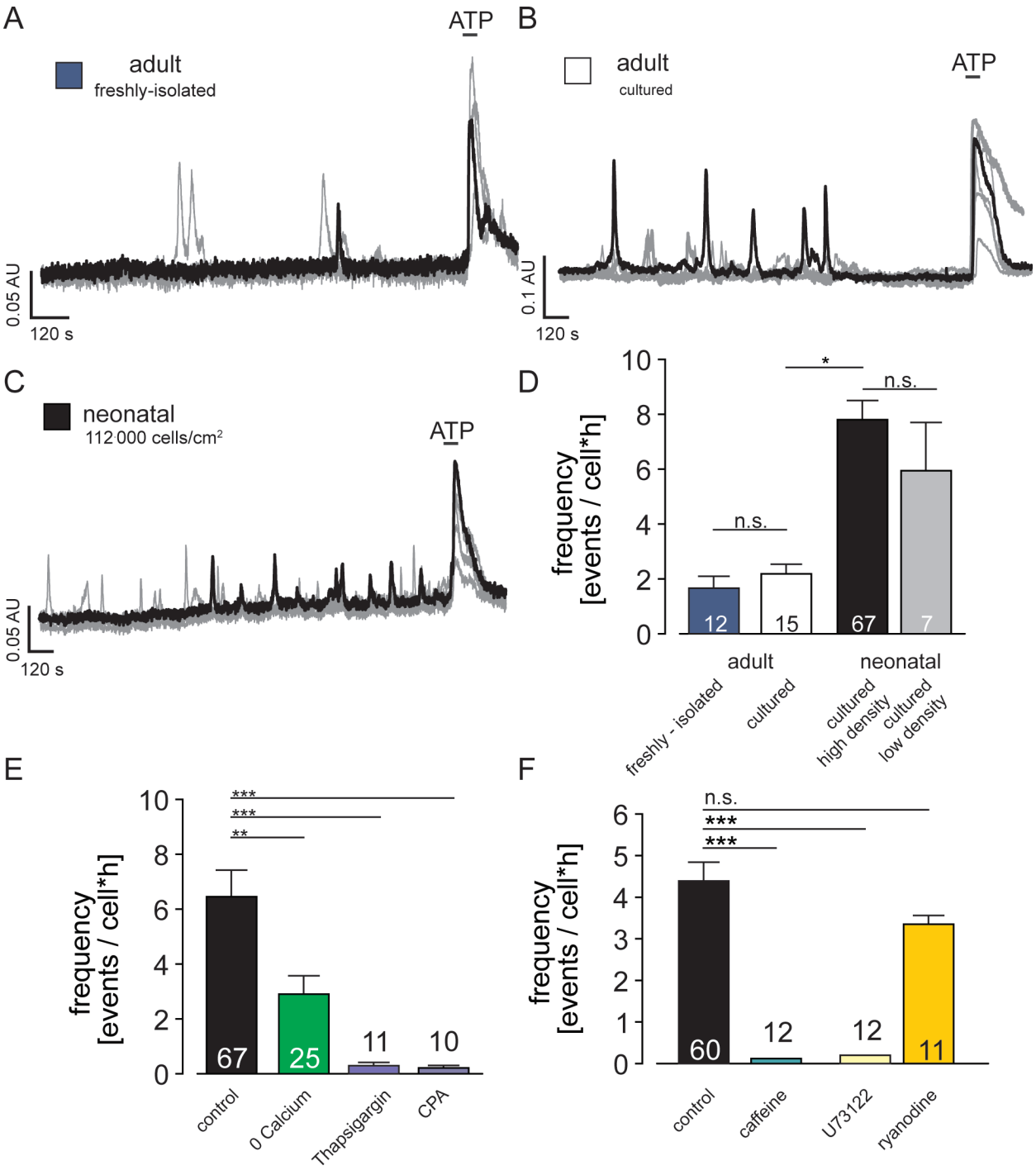

Figure 1: Spontaneous Ca^{2+} in microglia originate from the endoplasmic reticulum (A - C) Example recording of Fluo4-AM® loaded freshly isolated and primary cultured adult (8 - 12 weeks old) microglia and primary cultured neonatal (0 - 3 days old) microglia. The frequency of spontaneous Ca^{2+} events is lower in adult microglia compared to neonatal microglia (D). Inhibition of SERCA with Tg and CPA (E) and IP_3R with caffeine and U73122 abolished the spontaneous Ca^{2+} elevations in microglia, whereas inhibition of the ryanodine receptors with ryanodine had no effect. One - way ANOVA with Tukey *post hoc* testing. Statistics: n.s.: not significant; * $p < 0.05$; ** $p < 0.01$; *** $p < 0.001$; **** $p < 0.0001$. Numbers on the bars indicate the number of experiments (coverslips).

Internal Ca^{2+} stores regulate spontaneous Ca^{2+} transients To investigate this hypothesis SERCA was blocked with 2.5 μM Tg (7 culture preparations) or 20 μM CPA (3 culture preparations). Application of Tg (9.8 $\pm$ 4.1 %, n = 735 cells, 12 coverslips,

p = 4.7 * 10^{-5}) and CPA (0.1 $\pm$ 0.1 %, n = 766 cells, 10 coverslips, p = 6.1 * 10^{-6}) reduced the proportion of spontaneous active cells significantly compared to control (37.9 $\pm$ 3.2 %, n = 4389 cells, 58 coverslips). The frequency was 8 - fold reduced during Tg application (1.09 $\pm$ 0.24 events/cell * h, n = 682 cells, 11 coverslips, p = 0.01) and nearly absent after CPA application (0.21 $\pm$ 0.09 events/cell * h, n = 766 cells, 10 coverslips, p = 0.004, figure 1E). To determine the role of the Ca^{2+} release channels on the ER, neonatal cultured microglia were exposed to: (I) 10 mM caffeine, which activates RyRs but antagonizes IP_3Rs (4 culture preparations), (II) 20 μM U73122, which prevents IP_3 production via PLC (4 culture preparations), or (III) 20 μM ryanodine, which blocks RyR (3 culture preparations). The spontaneous Ca^{2+} events are mainly affected after inhibition of IP_3Rs (figure 1F). Furthermore, neonatal cultured microglia express mRNA for all 3 IP_3R isoforms, whereas they only express 1 ryanodine receptor isoform. Taken together, this data suggest that spontaneous Ca^{2+} events are mainly regulated via PLC, IP_3 and IP_3R.

Purinergic signalling does not trigger spontaneous Ca^{2+} events As microglia are well known for their purinergic signalling, it was hypothesized that the spontaneous Ca^{2+} transients could be triggered by these receptors. The ATP degradation pathway was accelerated in wild type neonatal cultured microglia by applying apyrase - an ATP degrading enzyme - (3 culture preparations) or delayed in ectonucleoside triphosphate diphophohydrolase - 1 (NTPDase1) knock-out animals ($CD39^{-/-}$, 4 culture preparations). Accelerating the process increased proportion (54.2 $\pm$ 6.1%, n = 257 cells, 14 coverslips,p = 8.4 * 10^{-6}) and frequency (20.9 $\pm$ 4.1 events/ cell * h, n = 185 cells, 8 coverslips, p = 3.96 * 10^{-3}) of the spontaneous events compared to control (24.7 $\pm$ 2.4%, n = 3265 cells, 61 coverslips and 10.5 $\pm$ 1.4 events/cell * hour, n = 2747 cells, 44 coverslips, 27 culture preparations). Whereas there was no difference between wild-type control and $CD39^{-/-}$ cultured microglia (33.1 $\pm$ 3.1%, n = 1587 cells, 46 coverslips, 11.5 $\pm$ 1.0 events/cell * h, n = 1290 cells, 33 coverslips).

To investigate the role of ATP release, microglia were incubated with 500 nM bafilomycin for 12 h to specifically inhibit the vesicular H^+ transporters (4 culture preparations). In addition, ATP could be release via large pore ion channels such as gap junctions and $P2X_7$ channels. As PPADS application increased the frequency it seems to be unlikely that ATP released via the $P2X_7$ plays a role in triggering spontaneous Ca^{2+} transients. The

gap junctions were blocked with 50 μM CBX (3 culture preparations). However, inhibiting the large pore ion channels with CBX or vesicle loading with bafilomycin had no affect on the proportion of cells displaying spontaneous activity ($p > 0.05$) or the frequency of spontaneous events ($p > 0.05$), suggesting that autocrine ATP release is not involved in triggering the spontaneous Ca^{2+} transients.

As a last step, the broad spectrum purinergic receptor antagonists RB2 (50 μM, 2 culture preparations), PPADS (100 μM) and suramin (100 μM, 4 culture preparations) and the metabotropic purinergic receptor (P2Y) 6 inhibitor MRS2578 (5 μM, 4 culture preparations) were applied in order to verify the general role of purinergic signalling in spontaneous Ca^{2+} transients. Surprisingly, inhibition of the purinergic receptors $P2Y_{4,\,6,\,12}$ with RB2 lead to high frequency Ca^{2+} oscillation with an unstable baseline. Therefore it was not possible to obtain reliable information about the spontaneous Ca^{2+} transients during RB2 application. Application of suramin, PPADS or MRS2578 did not affect the proportion of microglia displaying spontaneous Ca^{2+} events ($p > 0.05$). The frequency was, as indicated before, increased in frequency during PPADS application ($p < 1.0 * 10^{-6}$). Application of suramin or MRS2578 had no effect on the frequency of events. In summary, purinergic signalling can modulate the spontaneous Ca^{2+} events in microglia, but is not the main trigger for these events since inhibition of the purinergic receptors does not silence the spontaneous activity.

Pathological conditions alter the spontaneous Ca^{2+} transients Since microglia are part of the innate immune system in the central nervous system (CNS), we tested if spontaneous Ca^{2+} elevations are altered after an immune challenge, by either exposing them to LPS or during glioma development. LPS can be found on the membrane of gram - negative bacteria and are therefore recognized by microglia as a potential threat. For this experiment, 100 ng/ml LPS was applied in an acute (15 min during recording, 3 culture preparations) and 2 chronic (12 and 36 hours of stimulation, 3 culture preparations each) paradigms. These treatments did not alter the proportion of spontaneous active cells ($p > 0.05$) or the frequency of events ($p > 0.05$). Next, human (3 tumour preparations) and mouse (GL261-derived tumours, 3 animals) GAM where investigated for spontaneous calcium elevations. The proportion of cells displaying spontaneous Ca^{2+} was increased in human glioma - associated macrophages/ microglia (hGAM) (35.1 $\pm$ 5.7 %, n = 641 cells,

8 coverslips) compared to mouse glioma - associated macrophages/ microglia (mGAM) (13.8 $\pm$ 2.4 %, n = 423 cells, 9 coverslips, $p > 0.05$) or microglia extracted from the healthy mouse brain (14.4 $\pm$ 5.1 %, n = 228 cells, 12 coverslips, >0.05). The frequency of events was, however, not affected (p = 0.05). Thus, a larger proportion of hGAM display spontaneous activity compared to mGAM. Overall, the data suggests that spontaneous Ca^{2+} transients are not limited to mGAM but are also present in hGAM.

Project 1b: NMDA evoked Ca^{2+} elevations in microglia We showed that cortical spreading depression in acute cortical mouse brain slices promotes K^+ conductance in microglia cells and that this can be mimicked by NMDA bath application (Wendt et al., 2016). Previous reports on functional NMDAR remained, however, controversial (Kaindl et al., 2012; Murugan et al., 2011; Dissing-Olesen et al., 2014; Eyo et al., 2014). Therefore NMDA was directly applied to primary cultured adult microglia. S. Wendt was unable to detect NMDA triggered currents in microglia, whereas ATP was able to trigger a current in all recorded microglia (n = 23, figure 2A) in patch - clamp experiments. Therefore a similar experiment was preformed with Fluo4-AM® loaded microglia. In total, 10 coverslips were analysed but none of the cells displayed a Ca^{2+} increase during the NMDA wash - in phase whereas nearly all cells responded to ATP with a Ca^{2+} increase (figure 2B). It was therefore concluded that primary cultured adult microglia do not express functional NMDAR

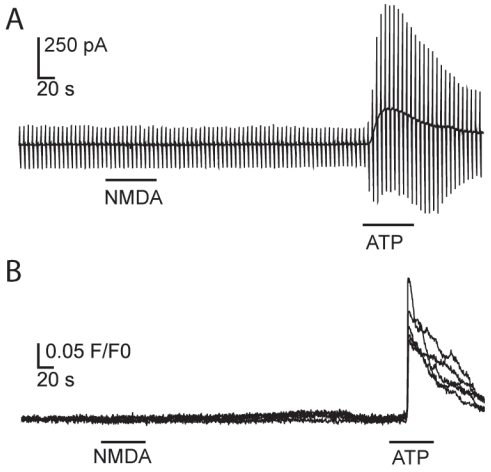

Figure 2: Microglia do not express functional NMDAR (A) Typical electro-physiological patch - clamp recording of a primary cultured adult microglia. Cells did not display a current upon exposure to 100 μM NMDA whereas 1 mM ATP triggered a current in all recorded microglia (n = 23). (B) Example recording of Fluo4-AM® loaded primary cultured adult microglia. The cells did not respond with a Ca^{2+} transient to NMDA when they were exposed to a similar stimulation protocol as with the electrophysiological recordings (n = 10 coverslips, 207 cells) Authors: A: S. Wendt, B: L. Korvers

1.3.2 Project 2: Functional recovery after prolonged neurotropic factor expression

Since neurotropic factors can direct neuronal outgrowth via Ca^{2+} signalling, prolonged neurotropic factor expression could enhance recovery after (sciatic) nerve injury. Therefore six candidate genes, of which their protein products signal via tyrosine kinase recep-

tors (CNTF, BDNF, GDNF, VEGF, NT - 3 and NGF) were over expressed in the auto-graft via transduction of a viral vector containing the construct. Motor (motion tracking) recovery of the rats was assessed over a period of 20 weeks to identify the most potential candidate neurotropic factor(s). Two rats, one from the VEGF and one from the CNTF group, were retrospectively excluded from further analysis since the sciatic nerve innervated a local muscle at the distal coaptation site.

To evaluate motor function recovery, the ankle angle was measured during toe off phase as the weight of the animal is pushed against gravity by the injured leg to start a new stance, requiring a significant amount of muscle strength during this phase. A minimum of four walking cycli were analysed from each individual rat to reduce variation in the walking cyclus of each individual. There was a severe drop in the ankle angle during toe off in the first 2 weeks after sciatic nerve injury. Bonferroni post hoc testing revealed that the ankle angles in GDNF treated animals were significantly smaller compared to sGFP treated animals during toe off at multiple time points (figure 3A). Thus the ankle angle in GDNF treated animals increase more slowly over time compared to sGFP treated animals during toe off. Marco - and microscopic inspection of the grafts 20 weeks post - surgery revealed that the graft was significantly enlarged (figure 3B) and contained a great number of motor neurons and Schwann cells, whereas the distal nerve end lacked re - innervating nerves and myelinated axons (figure 3C and D). None of the other neurotropic factors were capable of improving motor function recovery after injury compared to control.

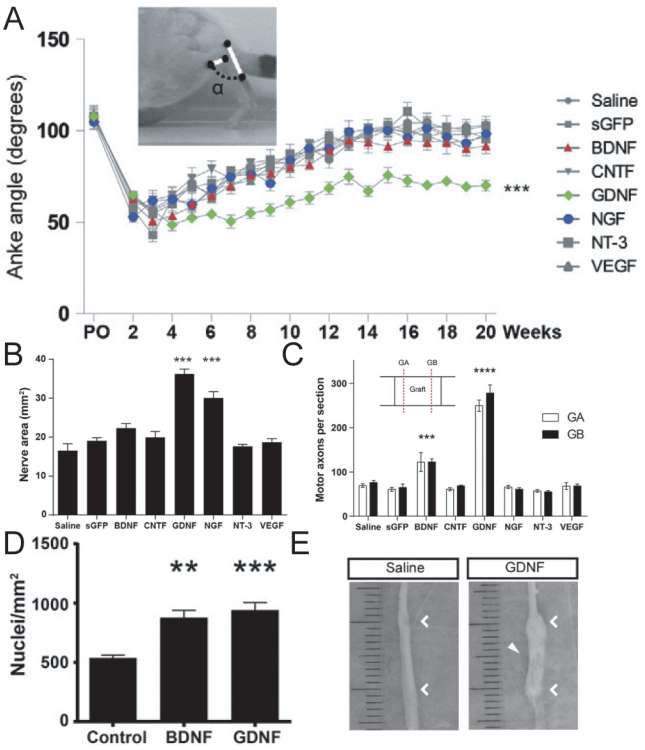

Figure 3: GDNF delays motor function recovery after sciatic nerve injury (A) Ankle angle of from the toe off phase followed over a 20 week period after sciatic nerve injury. GDNF delayed recovery, whereas none of the neurotropic factors were able to improve recovery. (B) Size of the graft taken from BDNF and GDNF treated animals is significantly enlarged after 20 weeks. This is probably caused by the increased number of motor axons at the proximal (GA) and distal (GB) end of the graft (C) and the increased number of cells (D). (E) Picture taken from the grafted area of saline treated control animals (left) and GDNF treated animals (right). The arrow marks the coaptation site of the graft. Statistics: n.s.: not significant; * $p < 0.05$; ** $p < 0.01$; *** $p < 0.001$; **** $p < 0.0001$. Numbers on the bars indicate the number of experiments (coverslips). Authors: A: L. Korvers, B - E: joint effort of S.A. Hoyng, F. de Winter and L. Korvers

1.4 Discussion

1.4.1 Project 1: Ca^{2+} signalling in microglia.

Project 1a: Spontaneous Ca^{2+} elevations in microglia Here we show microglia are capable of displaying spontaneous Ca^{2+} in various paradigms (cultured as well as freshly isolated) and conditions (LPS and glioma context). The spontaneous Ca^{2+} events are mainly regulated via PLC, IP_3, IP_3R and SERCA. External Ca^{2+} and purinergic receptor (P2) signalling can modulate the spontaneous Ca^{2+} events in microglia, but do not provide the triggering signal.

Considering that microglia maintain the spontaneous Ca^{2+} elevations under all conditions and the occurrence is highly linked to the ER, which is not only a major internal Ca^{2+} storage facility but also involved in protein processing, it could be possible that theses elevations maintain basic microglia function. Indeed, it has been shown by Dolmetsch et al. (1998) that gene expression in cells can be manipulated by frequency and amplitude of the Ca^{2+} increases. Further more, the luminal Ca^{2+} concentration in the ER and cytosolic ATP concentrations can modulate IP_3R function, supporting Ca^{2+} oscillations (Thrower et al., 2000). And last, but not least the ER interacts closely with the mitochondria (Naon and Scorrano, 2014), allowing close manipulation of ATP production (Denton, 2009). Taken these observations in consideration, the increased rise and decay times of the spontaneous Ca^{2+} transients after LPS stimulation or the reduced rise and decay times in mGAM could result in/ reflect the altered gene expression in microglia under these conditions (Szulzewsky et al., 2015).

Project 1b: NMDA evoked Ca^{2+} elevations in microglia We observed that microglia increase their K^+ conductance during cortical spreading depression *in situ*. This observation could be mimicked by NMDA application. Although *in vitro* application of NMDAR inhibitors is toxic for microglia (Hirayama and Kuriyama, 2001) and can express NMDAR subunits (Murugan et al., 2011), there is no evidence so far for the expression of functional NMDAR *in situ* microglia. In our hands, application of NMDA to primary cultured adult microglia did not increase membrane conductance or a Ca^{2+} response. Although functional NMDAR expression could depend on environmental conditions and/ or age, we propose that the increased K^+ conductance in cortical acute brains slice resident microglia upon NMDA application *in situ* is an indirect result of neuron - microglia signalling.

1.4.2 Project 2: Functional recovery after prolonged neurotropic factor expression

Neurotropic factors can induce gene expression via increasing intracellular Ca^{2+} concentrations. Six neurotropic factors (CNTF, BDNF, GDNF, VEGF, NT - 3 and NGF) were virally expressed in sciatic nerve auto - grafts to maintain the growth promoting environment after nerve lesion. In a 20 week follow - up study, it was observed that motor function recovery was delayed in GDNF treated animals, whereas other neurotropic did not enhance recovery compared to control. This is probably caused by the increased number of motor axons and Schwann cells in the graft and the lack of neuron innervation and axon myelination in the distal nerve.

What has to be taken in careful consideration with these experiments is that expression and processing of neurotropic factors is tightly regulated within specific cells. In other words, most of the neurotropic factors have multiple splice variants which are expressed in specific cell types, meaning that the gene promoter contains detailed information about gene regulation (Brushart, 2011). This specific and important information is lost by placing the gene encoding for the neurotropic factor in a viral vector regulated by the CMV promoter. Thus all cells within the graft will express the neurotropic factor all the time instead of a few selected cells in specific time intervals which prevents coordinated and guided regrowth of the axons. Therefore it is important to develop a strategy using an cell specific inducible gene expression system.

References

Bruce Alberts, Alexander Johnson, Julian Lewis, Martin Raff, Keith Roberts, and Peter Walter. Signaling through Enzyme-Linked Cell-Surface Receptors. 2002.

Peter H. Barry and Joseph W. Lynch. Ligand-gated channels. *IEEE transactions on nanobioscience*, 4(1):70–80, March 2005. ISSN 1536-1241.

Danya Ben-Hail, Raz Palty, and Varda Shoshan-Barmatz. Measurement of Mitochondrial Ca2+ Transport Mediated by Three Transport Proteins: VDAC1, the Na+/Ca2+ Exchanger, and the Ca2+ Uniporter. *Cold Spring Harbor Protocols*, 2014(2):pdb.top066241, January 2014. ISSN 1940-3402, 1559-6095. doi: 10.1101/pdb.top066241.

Hans Bräuner-Osborne, Petrine Wellendorph, and Anders A. Jensen. Structure, pharmacology and therapeutic prospects of family C G-protein coupled receptors. *Current Drug Targets*, 8(1):169–184, January 2007. ISSN 1873-5592.

Bianca Brawek, Bernd Schwendele, Karin Riester, Shinichi Kohsaka, Chommanad Lerdkrai, Yajie Liang, and Olga Garaschuk. Impairment of in vivo calcium signaling in amyloid plaque-associated microglia. *Acta Neuropathologica*, 127(4):495–505, January 2014. ISSN 0001-6322, 1432-0533. doi: 10.1007/s00401-013-1242-2.

Paul S. Brookes, Yisang Yoon, James L. Robotham, M. W. Anders, and Shey-Shing Sheu. Calcium, ATP, and ROS: A mitochondrial love-hate triangle. *American Journal of Physiology - Cell Physiology*, 287(4):C817–C833, October 2004. ISSN 0363-6143, 1522-1563. doi: 10.1152/ajpcell.00139.2004.

Thomas M. Brushart. *Nerve Repair*. Oxford University Press, February 2011. ISBN 978-0-19-972160-3. Google-Books-ID: RNQIfsA2iUUC.

Geoffrey Burnstock and Alexei Verkhratsky. *Purinergic Signalling and the Nervous System*. Springer Berlin Heidelberg, Berlin, Heidelberg, 2012. ISBN 978-3-642-28862-3 978-3-642-28863-0.

Diego De Stefani, Maria Patron, and Rosario Rizzuto. Structure and function of the mitochondrial calcium uniporter complex. *Biochimica et Biophysica Acta (BBA) - Molecular Cell Research*, 1853(9):2006–2011, September 2015. ISSN 0167-4889. doi: 10.1016/j.bbamcr.2015.04.008.

P. Del Rio Hortega. El tercer elemento de los centros nerviosos. *Bol. Soc. Esp. Biol*, 9: 69–129, 1919.

Richard M. Denton. Regulation of mitochondrial dehydrogenases by calcium ions. *Biochimica et Biophysica Acta (BBA) - Bioenergetics*, 1787(11):1309–1316, November 2009. ISSN 0005-2728. doi: 10.1016/j.bbabio.2009.01.005.

Lasse Dissing-Olesen, Jeffrey M. LeDue, Ravi L. Rungta, Jasmin K. Hefendehl, Hyun B. Choi, and Brian A. MacVicar. Activation of neuronal NMDA receptors triggers transient ATP-mediated microglial process outgrowth. *The Journal of Neuroscience: The Official Journal of the Society for Neuroscience*, 34(32):10511–10527, August 2014. ISSN 1529-2401. doi: 10.1523/JNEUROSCI.0405-14.2014.

R E Dolmetsch, K Xu, and R S Lewis. Calcium oscillations increase the efficiency and specificity of gene expression. *Nature*, 392(6679):933–936, April 1998. ISSN 0028-0836. doi: 10.1038/31960.

Geneviève Dupont, Laurent Combettes, Gary S. Bird, and James W. Putney. Calcium Oscillations. *Cold Spring Harbor Perspectives in Biology*, 3(3):a004226, January 2011. ISSN , 1943-0264. doi: 10.1101/cshperspect.a004226.

Gerhard Eichhoff, Bianca Brawek, and Olga Garaschuk. Microglial calcium signal acts as a rapid sensor of single neuron damage in vivo. *Biochimica et Biophysica Acta (BBA) - Molecular Cell Research*, 1813(5):1014–1024, May 2011. ISSN 0167-4889. doi: 10.1016/j.bbamcr.2010.10.018.

Ukpong B. Eyo, Jiyun Peng, Przemyslaw Swiatkowski, Aparna Mukherjee, Ashley Bispo, and Long-Jun Wu. Neuronal hyperactivity recruits microglial processes via neuronal NMDA receptors and microglial P2Y12 receptors after status epilepticus. *The Journal of Neuroscience: The Official Journal of the Society for Neuroscience*, 34(32):10528–10540, August 2014. ISSN 1529-2401. doi: 10.1523/JNEUROSCI.0416-14.2014.

Wolfgang F. Graier, Maud Frieden, and Roland Malli. Mitochondria and Ca2+ signaling: Old guests, new functions. *Pflügers Archiv - European Journal of Physiology*, 455(3): 375–396, July 2007. ISSN 0031-6768, 1432-2013. doi: 10.1007/s00424-007-0296-1.

M. Hirayama and M. Kuriyama. MK-801 is cytotoxic to microglia in vitro and its cytotoxicity is attenuated by glutamate, other excitotoxic agents and atropine. Possible presence of glutamate receptor and muscarinic receptor on microglia. *Brain Research*, 897(1-2): 204–206, April 2001. ISSN 0006-8993.

Brian L. Jones and Stephen M. Smith. Calcium-Sensing Receptor: A Key Target for

Extracellular Calcium Signaling in Neurons. *Frontiers in Physiology*, 7, March 2016. ISSN 1664-042X. doi: 10.3389/fphys.2016.00116.

Yue-Kun Ju, Elizabeth A. Woodcock, David G. Allen, and Mark B. Cannell. Inositol 1,4,5-trisphosphate receptors and pacemaker rhythms. *Journal of Molecular and Cellular Cardiology*, 53(3):375–381, September 2012. ISSN 0022-2828. doi: 10.1016/j.yjmcc.2012.06.004.

Angela M. Kaindl, Vincent Degos, Stéphane Peineau, Elodie Gouadon, Vibol Chhor, Gauthier Loron, Tifenn Le Charpentier, Julien Josserand, Carine Ali, Denis Vivien, Graham L. Collingridge, Alain Lombet, Lina Issa, Frédérique Rene, Jean-Philippe Loeffler, Annemieke Kavelaars, Catherine Verney, Jean Mantz, and Pierre Gressens. Activation of microglial N-methyl-D-aspartate receptors triggers inflammation and neuronal cell death in the developing and mature brain. *Annals of Neurology*, 72(4):536–549, October 2012. ISSN 1531-8249. doi: 10.1002/ana.23626.

Helmut Kettenmann, Uwe-Karsten Hanisch, Mami Noda, and Alexei Verkhratsky. Physiology of Microglia. *Physiological Reviews*, 91(2):461–553, January 2011. ISSN 0031-9333, 1522-1210. doi: 10.1152/physrev.00011.2010.

Johanna T. Lanner, Dimitra K. Georgiou, Aditya D. Joshi, and Susan L. Hamilton. Ryanodine Receptors: Structure, Expression, Molecular Details, and Function in Calcium Release. *Cold Spring Harbor Perspectives in Biology*, 2(11):a003996, January 2010. ISSN , 1943-0264. doi: 10.1101/cshperspect.a003996.

Madhuvika Murugan, Viswanathan Sivakumar, Jia Lu, Eng-Ang Ling, and Charanjit Kaur. Expression of N-methyl D-aspartate receptor subunits in amoeboid microglia mediates production of nitric oxide via NF-κB signaling pathway and oligodendrocyte cell death in hypoxic postnatal rats. *Glia*, 59(4):521–539, April 2011. ISSN 1098-1136. doi: 10.1002/glia.21121.

Deborah Naon and Luca Scorrano. At the right distance: ER-mitochondria juxtaposition in cell life and death. *Biochimica Et Biophysica Acta*, May 2014. ISSN 0006-3002. doi: 10.1016/j.bbamcr.2014.05.011.

Maria Nikodemova and Jyoti J. Watters. Efficient isolation of live microglia with preserved phenotypes from adult mouse brain. *Journal of Neuroinflammation*, 9:147, 2012. ISSN 1742-2094. doi: 10.1186/1742-2094-9-147.

Muthu Periasamy and Anuradha Kalyanasundaram. SERCA pump isoforms: Their role

in calcium transport and disease. *Muscle & Nerve*, 35(4):430–442, April 2007. ISSN 1097-4598. doi: 10.1002/mus.20745.

Jennifer M Pocock and Helmut Kettenmann. Neurotransmitter receptors on microglia. *Trends in Neurosciences*, 30(10):527–535, October 2007. ISSN 0166-2236. doi: 10.1016/j.tins.2007.07.007.

Amir Pozner, Ben Xu, Sierra Palumbos, J. Michael Gee, Petr Tvrdik, and Mario R. Capecchi. Intracellular calcium dynamics in cortical microglia responding to focal laser injury in the PC::G5-tdT reporter mouse. *Frontiers in Molecular Neuroscience*, 8, May 2015. ISSN 1662-5099. doi: 10.3389/fnmol.2015.00012.

Daniel Prins and Marek Michalak. Organellar Calcium Buffers. *Cold Spring Harbor Perspectives in Biology*, 3(3):a004069, January 2011. ISSN , 1943-0264. doi: 10.1101/cshperspect.a004069.

Bruce R. Ransom and Helmut Kettenmann. *Neuroglia*. Oxford University Press USA, 4 edition, December 2012. ISBN 0-19-979459-6.

Jane B. Reece, Lisa A. Urry, Michael L. Cain, Steven A. Wasserman, Peter V. Minorsky, Robert B. Jackson, and Neil A. Campbell. *Biology*. Number 9 in Campbell Biology. Benjamin Cummings, October 2010. ISBN 0-321-55823-5.

Rosario Rizzuto, Saverio Marchi, Massimo Bonora, Paola Aguiari, Angela Bononi, Diego De Stefani, Carlotta Giorgi, Sara Leo, Alessandro Rimessi, Roberta Siviero, Erika Zecchini, and Paolo Pinton. Ca2+ transfer from the ER to mitochondria: When, how and why. *Biochimica et Biophysica Acta (BBA) - Bioenergetics*, 1787(11):1342–1351, November 2009. ISSN 0005-2728. doi: 10.1016/j.bbabio.2009.03.015.

Isabelle Rousse and Richard Robitaille. Calcium signaling in Schwann cells at synaptic and extra-synaptic sites: Active glial modulation of neuronal activity. *Glia*, 54(7):691–699, November 2006. ISSN 1098-1136. doi: 10.1002/glia.20388.

R A Segal, Greenberg, and M. E. Intracellular Signaling Pathways Activated by Neuropathic Factors. *Annual Review of Neuroscience*, 19(1):463–489, 1996. doi: 10.1146/annurev.ne.19.030196.002335.

Purnima Sharma and Liao Ping. Calcium ion influx in microglial cells: Physiological and therapeutic significance. *Journal of Neuroscience Research*, 92(4):409–423, April 2014. ISSN 1097-4547. doi: 10.1002/jnr.23344.

Amanda Sierra, Juan M. Encinas, Juan J. P. Deudero, Jessica H. Chancey, Grig-

ori Enikolopov, Linda S. Overstreet-Wadiche, Stella E. Tsirka, and Mirjana Maletic-Savatic. Microglia shape adult hippocampal neurogenesis through apoptosis-coupled phagocytosis. *Cell Stem Cell*, 7(4):483–495, October 2010. ISSN 1875-9777. doi: 10.1016/j.stem.2010.08.014.

Frank Szulzewsky, Andreas Pelz, Xi Feng, Michael Synowitz, Darko Markovic, Thomas Langmann, Inge R. Holtman, Xi Wang, Bart J. L. Eggen, Hendrikus W. G. M. Boddeke, Dolores Hambardzumyan, Susanne A. Wolf, and Helmut Kettenmann. Glioma-Associated Microglia/Macrophages Display an Expression Profile Different from M1 and M2 Polarization and Highly Express Gpnmb and Spp1. *PLoS ONE*, 10(2), February 2015. ISSN 1932-6203. doi: 10.1371/journal.pone.0116644.

Edwin C. Thrower, Hamid Mobasheri, Sheila Dargan, Phedra Marius, Edward J. A. Lea, and Alan P. Dawson. Interaction of Luminal Calcium and Cytosolic ATP in the Control of Type 1 Inositol (1,4,5)-Trisphosphate Receptor Channels. *Journal of Biological Chemistry*, 275(46):36049–36055, November 2000. ISSN 0021-9258, 1083-351X. doi: 10.1074/jbc.M000970200.

Stefan Wendt, Emile Wogram, Laura Korvers, and Helmut Kettenmann. Experimental Cortical Spreading Depression Induces NMDA Receptor Dependent Potassium Currents in Microglia. *The Journal of Neuroscience: The Official Journal of the Society for Neuroscience*, 36(23):6165–6174, June 2016. ISSN 1529-2401. doi: 10.1523/JNEUROSCI.4498-15.2016.

Gerald W. Zamponi, Joerg Striessnig, Alexandra Koschak, and Annette C. Dolphin. The Physiology, Pathology, and Pharmacology of Voltage-Gated Calcium Channels and Their Future Therapeutic Potential. *Pharmacological Reviews*, 67(4):821–870, October 2015. ISSN 1521-0081. doi: 10.1124/pr.114.009654.

2 Affidavit

I, Laura Maria Korvers, certify under penalty of perjury by my own signature that I have submitted the thesis on the topic calcium signalling in the nervous system. I wrote this thesis independently and without assistance from third parties, I used no other aids than the listed sources and resources.

All points based literally or in spirit on publications or presentations of other authors are, as such, in proper citations (see "uniform requirements for manuscripts (URM)" the ICMJE www.icmje.org) indicated. The sections on methodology (in particular practical work, laboratory requirements, statistical processing) and results (in particular images, graphics and tables) correspond to the URM (s.o) and are answered by me. My interest in any publications to this dissertation correspond to those that are specified in the following joint declaration with the responsible person and supervisor. All publications resulting from this thesis and which I am author correspond to the URM (see above) and I am solely responsible.

The importance of this affidavit and the criminal consequences of a false affidavit (section 156,161 of the Criminal Code) are known to me and I understand the rights and responsibilities stated therein.

Date Signature

27.10.2016

Berlin Laura Korvers

2.1 Declaration of any eventual publications

Laura Maria Korvers had the following share in the following publications:

Publication 1:
Laura Korvers, Amanda de Andrade Costa, Martin Mersch, Vitali Matyash, Helmut Kettenmann and Marcus Semtner Spontaneous Ca^{2+} transients in mouse microglia
Cell Calcium 2016 Dec, 60 (6);396 - 400

Contribution in detail:

1. Writing customized Igor Pro script for data analysis
2. Treatment of primary cultured neonatal microglia with LPS and bafilomycin A_1
3. Live cell Ca^{2+} imaging of primary cultured neonatal and adult microglia and freshly isolated microglia (wild type and mouse glioma - associated macrophages/ microglia)
4. Video analysis of primary cultured neonatal and adult microglia, freshly isolated microglia and human glioma - associated macrophages/ microglia.

Publication 2:
Wendt S, Wogram E, Korvers L, Kettenmann H. Experimental Cortical Spreading Depression Induces NMDA Receptor Dependent Potassium Currents in Microglia.
J Neurosci. 2016 Jun 8;36(23):6165-74

Contribution in detail:

1. Live cell Ca^{2+} imaging
2. Analysis of Ca^{2+} response to NMDA

Publication 3:

Hoyng SA, De Winter F, Gnavi S, de Boer R, Boon LI, Korvers LM, Tannemaat MR, Malessy MJ, Verhaagen J. A comparative morphological, electrophysiological and functional analysis of axon regeneration through peripheral nerve autografts genetically modified to overexpress BDNF, CNTF, GDNF, NGF, NT3 or VEGF. Exp Neurol. 2014 Nov;261:578-93.

Contribution in detail:

1. Recording motor recovery in rats in a 20 week follow up study.
2. Analysis of motor tracking video's
3. Sectioning of sciatic nerve and anti - body testing for immuno - histochemical staining.

Signature, date and stamp of the supervising University teacher

Signature of the doctoral candidate

Laura Korvers

3 Publications

Spontaneous Ca^{2+} transients in mouse microglia.

Korvers L, de Andrade Costa A, Mersch M, Matyash V, Kettenmann H, Semtner M. Cell Calcium. 2016 Dec;60(6):396-406. doi: 10.1016/j.ceca.2016.09.004. Epub 2016 Sep 22. Spontaneous Ca^{2+} transients in mouse microglia.

https://doi.org/10.1016/j.ceca.2016.09.004

Spontaneous Ca^{2+} transients in mouse microglia.

Korvers L, de Andrade Costa A, Mersch M, Matyash V, Kettenmann H, Semtner M. Cell Calcium. 2016 Dec;60(6):396-406. doi: 10.1016/j.ceca.2016.09.004. Epub 2016 Sep 22. Spontaneous Ca^{2+} transients in mouse microglia.

https://doi.org/10.1016/j.ceca.2016.09.004

Spontaneous Ca^{2+} transients in mouse microglia.

Korvers L, de Andrade Costa A, Mersch M, Matyash V, Kettenmann H, Semtner M. Cell Calcium. 2016 Dec;60(6):396-406. doi: 10.1016/j.ceca.2016.09.004. Epub 2016 Sep 22. Spontaneous Ca^{2+} transients in mouse microglia.

https://doi.org/10.1016/j.ceca.2016.09.004

Spontaneous Ca^{2+} transients in mouse microglia.

Korvers L, de Andrade Costa A, Mersch M, Matyash V, Kettenmann H, Semtner M. Cell Calcium. 2016 Dec;60(6):396-406. doi: 10.1016/j.ceca.2016.09.004. Epub 2016 Sep 22. Spontaneous Ca^{2+} transients in mouse microglia.

https://doi.org/10.1016/j.ceca.2016.09.004

Spontaneous Ca^{2+} transients in mouse microglia.

Korvers L, de Andrade Costa A, Mersch M, Matyash V, Kettenmann H, Semtner M. Cell Calcium. 2016 Dec;60(6):396-406. doi: 10.1016/j.ceca.2016.09.004. Epub 2016 Sep 22. Spontaneous Ca^{2+} transients in mouse microglia.

https://doi.org/10.1016/j.ceca.2016.09.004

Spontaneous Ca^{2+} transients in mouse microglia.

Korvers L, de Andrade Costa A, Mersch M, Matyash V, Kettenmann H, Semtner M. Cell Calcium. 2016 Dec;60(6):396-406. doi: 10.1016/j.ceca.2016.09.004. Epub 2016 Sep 22. Spontaneous Ca^{2+} transients in mouse microglia.

https://doi.org/10.1016/j.ceca.2016.09.004

Spontaneous Ca^{2+} transients in mouse microglia.

Korvers L, de Andrade Costa A, Mersch M, Matyash V, Kettenmann H, Semtner M. Cell Calcium. 2016 Dec;60(6):396-406. doi: 10.1016/j.ceca.2016.09.004. Epub 2016 Sep 22. Spontaneous Ca^{2+} transients in mouse microglia.

https://doi.org/10.1016/j.ceca.2016.09.004

Spontaneous Ca^{2+} transients in mouse microglia.

Korvers L, de Andrade Costa A, Mersch M, Matyash V, Kettenmann H, Semtner M. Cell Calcium. 2016 Dec;60(6):396-406. doi: 10.1016/j.ceca.2016.09.004. Epub 2016 Sep 22. Spontaneous Ca^{2+} transients in mouse microglia.

https://doi.org/10.1016/j.ceca.2016.09.004

Spontaneous Ca^{2+} transients in mouse microglia.

Korvers L, de Andrade Costa A, Mersch M, Matyash V, Kettenmann H, Semtner M. Cell Calcium. 2016 Dec;60(6):396-406. doi: 10.1016/j.ceca.2016.09.004. Epub 2016 Sep 22. Spontaneous Ca^{2+} transients in mouse microglia.

https://doi.org/10.1016/j.ceca.2016.09.004

Spontaneous Ca^{2+} transients in mouse microglia.

Korvers L, de Andrade Costa A, Mersch M, Matyash V, Kettenmann H, Semtner M. Cell Calcium. 2016 Dec;60(6):396-406. doi: 10.1016/j.ceca.2016.09.004. Epub 2016 Sep 22. Spontaneous Ca^{2+} transients in mouse microglia.

https://doi.org/10.1016/j.ceca.2016.09.004

Spontaneous Ca^{2+} transients in mouse microglia.

Korvers L, de Andrade Costa A, Mersch M, Matyash V, Kettenmann H, Semtner M. Cell Calcium. 2016 Dec;60(6):396-406. doi: 10.1016/j.ceca.2016.09.004. Epub 2016 Sep 22. Spontaneous Ca^{2+} transients in mouse microglia.

https://doi.org/10.1016/j.ceca.2016.09.004

Experimental cortical spreading depression induces NMDA receptor dependent potassium currents in microglia

Stefan Wendt[1], Emile Wogram[1,2], Laura Korvers[1] and Helmut Kettenmann[1]
[1] Cellular Neurosciences, Max-Delbrück Center for Molecular Medicine, 13092 Berlin, Germany
[2] Institute of Physiology and Pathophysiology, University of Heidelberg, 69120 Heidelberg, Germany

Keyword suggestions: microglia; potassium channels; spreading depression; NMDA receptor

For correspondence:
Prof. Dr. Helmut Kettenmann
Cellular Neurosciences
Max Delbrueck Center for Molecular Medicine in the Helmholtz Society
Robert-Roessle-Strasse 10
13125 Berlin
Germany
kettenmann@mdc-berlin.de

Abstract

Cortical spreading depression (CSD) is a propagating event of neuronal depolarization which is considered as the cellular correlate of the migraine aura. It is characterized by a change in the intrinsic optical signal and by a negative DC potential shift. Microglia are the resident macrophages of the central nervous system and act as sensors for pathological changes. In the present study we analyzed whether microglial cells might sense CSD by recording membrane currents from microglia in acutely isolated cortical mouse brain slices during an experimentally induced CSD. Coincident with the change in the intrinsic optical signal and the negative DC potential shift we recorded an increase in potassium conductance predominantly mediated by $K_{ir}2.1$ which was blocked by the NMDA receptor antagonist D-AP5. Application of NMDA and an increase in extracellular K^+ mimics the CSD induced K_{ir} activation. Application of D-AP5, but not the purinergic receptor antagonist RB2, blocks the NMDA induced K_{ir} activation. The K^+ channel blocker Ba^{2+} blocks both, the CSD and the NMDA triggered increase in K_{ir} channel activity. In addition we could confirm previous findings that microglia in the adult brain do not express functional NMDA receptors by recording from microglia cultured from adult brain. From these observations we conclude that CSD activates neuronal NMDA receptors which lead to an increase in extracellular $[K^+]$ resulting in the activation of K_{ir} channel activity in microglia.

Acknowledgements

This work was supported by Deutsche Forschungsgemeinschaft (SFB TRR43, EXC 257 NeuroCure). We thank Vitali Matyash for discussion and Niklas Meyer for experimental help. For technical assistance we would like to thank Regina Piske and Maren Wendt. In addition we would like to thank Ulrike Pannasch for project ideas. The authors declare no competing financial interests.

Significance statement

Cortical spreading depression (CSD) is a wave of neuronal depolarization spreading through the cortex and is associated with the aura of migraine. Here we show that microglial cells, which are viewed as pathologic sensors of the brain, can sense this wave. The increase in the extracellular potassium concentration associated with that wave leads to the activation of an inward rectifying potassium conductance in microglia. The involvement of neuronal NMDA receptors is crucial since NMDA mimics that response and microglia do not express functional NMDA receptors. While it is now evident that CSD leads to a signal in microglia, the consequences of this microglial activation during CSD needs to be explored.

Introduction

Microglial cells are the immunocompetent cells of the central nervous system. They are characterized by a distinct ramified morphology with small cell bodies and branched processes which constantly scan the environment and contact surrounding neurons (Nimmerjahn et al., 2005; Kettenmann et al., 2011). In the pathologic brain microglia undergo a rapid transformation acquiring an amoeboid morphology and can, depending on the state of activation, release cytokines, phagocytose, proliferate or migrate (Hanisch and Kettenmann, 2007). In excitotoxic pathologies like epilepsy microglia are also activated due to increased neuronal activity (Avignone et al., 2015). Another event involving temporally increased neuronal activity followed by decreased activity is known as cortical spreading depression (CSD), discovered in 1944 (Leão, 1944). It is characterized by a slowly propagating (3 - 4 mm/min) wave of neuronal and glial depolarization followed by a period of neuronal depression. It is considered to be the cellular counterpart of migraine aura (Lauritzen, 1992). Hallmarks of these depolarizing

waves are neuronal swelling, a negative DC potential shift, elevation of extracellular potassium and glutamate leading to disturbed ion homeostasis (Dreier, 2011). Propagation of CSD requires NMDA receptor activation and can be blocked by NMDA receptor antagonists (Marrannes et al., 1988; Lauritzen and Hansen, 1992). Whether microglial cells sense the state of neuronal activity in pathologies like CSD is not known. Microglia express neurotransmitter receptors such as AMPA and metabotropic glutamate receptors which might be means to sense excitotoxicity (Kettenmann et al., 2011). While the expression of functional NMDA receptors has been described for cultured neonatal microglial cells (Kaindl et al., 2012) their presence *in situ* could not be confirmed (Dissing-Olesen *et al.*, 2014; Eyo *et al.*, 2014). In the present study we tested the influence of CSD on microglial membrane conductance in acute mouse brain slices. Our results indicate that microglia can sense NMDA receptor dependent potassium elevations during CSD by an increase in potassium inward rectifier activity and we confirm the lack of functional NMDA receptor expression in microglia.

Material and Methods

Solutions

For experiments in cell culture a standard HEPES buffer was used containing (in mM): NaCl 150; KCL 5.4; $MgCl_2$ 1; $CaCl_2$ 2; HEPES 10 and glucose 10 adjusted to a pH of 7.4 with NaOH. As extracellular solution and for preparation of brain slices the following artificial cerebrospinal fluid (ACSF) was used (in mM): NaCl, 134; KCl, 2.5; $MgCl_2$, 1.3; $CaCl_2$, 2; K_2HPO_4, 1.25; $NaHCO_3$, 26; D-glucose, 10; pH 7.4; with osmolarity of 310 - 320 mOsm/L and gassed with 95 % O_2/ 5 % CO_2. For electrophysiological recordings the following intracellular solution was used (in mM): NaCl 130; $MgCl_2$ 2; $CaCl_2$, 0.5; Na-ATP, 2; EGTA, 5; HEPES, 10; and sulforhodamine 101, 0.01 (SR101) (Sigma Aldrich, St. Louis, USA) with an osmolarity of 280 - 290 mOsm/L adjusted to a pH of 7.3 with KOH. The following substances were added into the HEPES buffer or ACSF for pharmacological approaches (in mM): ATP 1 (Sigma Aldrich); $BaCl_2$ 1 (Sigma Aldrich); CNQX 0.01 (Tocris, Bristol, UK); D-AP5 0.05 (Abcam, Cambridge, UK); Glibenclamide 0.1 (Tocris); NMDA 0.1 (Tocris); Nortriptyline 0.1 (Sigma Aldrich); ML133 0.02 (Sigma Aldrich); Reactive Blue 2 0.1 (Tocris); Tertiapin-Q 0.2 $*10^{-3}$ (Tocris); VU590 0.01 (Sigma Aldrich). Changed magnesium or potassium concentrations were substituted with equimolar NaCl.

Animals

All mice used for the present study were on a C57BL/6 genetic background of both sexes. For preparation of cultured cells wildtype animals were used whereas mice for electrophysiological recordings contained a *Csf1r*-EGFP tag (MacGreen). For acute brain slice preparation mice were used at an age of P42 – 63. Animals were kept according to the German law for animal protection under a 12 hour/12 hour dark-light cycle with food and water supply *ad libitum*.

Neonatal microglia cell culture:

Neonatal primary microglia cultures were obtained from cerebral cortex and midbrain using P0 to P3 mice (Giulian and Baker, 1986). Microglia were seeded with 3 – 5 10 x 10^5 cells on glass coverslips.

Adult microglia cell culture:

Primary adult microglia cultures were prepared as described before using P49 to P56 mice (Scheffel et al., 2012). In short, the cerebellum and olfactory bulb were removed and the cerebrum was freed of blood vessels and meninges and stored in Hank's balanced salt solution (HBBS). Subsequently the tissue was chopped down to 1 mm^3 pieces and trypsinized in 1 % trypsin and 0.05 % deoxyribonuclease for 5 min at room temperature. Using a fire-polished pipette the tissue was dissociated and washed twice in HBBS. Cell suspension was plated on a confluent monolayer of neonatal astrocytes in 75 cm^2 flasks. Clodronate (200 µg/mL) was used to remove neonatal microglial cells before adding the adult cell suspension. DMEM was used to culture the mixed glial cells and medium was changed in a daily routine. After 7 days 33 % L929-conditioned medium was added and after another 7 days microglial cells were shaken off for experiments. Cell suspension was transferred on cover slips in a single droplet containing 5 - 10 x 10^5 cells. Coverslips were used for calcium imaging and patch-clamp recordings one day after plating.

Preparation of acute mouse brain slices:

Acute mouse brain slices were prepared as described earlier (Boucsein et al., 2003). Briefly, mice were sacrificed via dislocation of the vertebra. The brain was removed and placed in ice cold ACSF adjusted to a pH of 7.4. Using a microtome, 250 – 350 µm thick coronal brain slices were made and kept in gassed ACSF at room temperature. Experiments were done within a maximum of 5 hours.

Electrophysiological recordings:

The whole-cell patch-clamp technique was employed to study membrane currents of microglia *in situ* and *in vitro*. Brain slices and cover slips were superfused at 3 – 6 mL/min with ACSF or HEPES buffer at room temperature. Pipettes were pulled from borosilicate glasses with a resistance of 4 - 6 MΩ. After establishing the whole cell recording configuration, only cells with a series resistance below 65 MΩ were used. A series of de- and hyperpolarizing 100 ms pulses were applied ranging from -140 to 60 mV with 20 mV increment from a holding potential of -20 mV in voltage clamp mode. This protocol was repeated every 5 s to allow continuous monitoring of microglial membrane currents and current voltage relationships. For illustration the traces were filtered with a 5 - 8 Hz low pass Bessel filter. For field potential recordings glass pipettes with a resistance of ~1 MΩ were placed at 20 – 50 µm depth in the slice. All recordings were done with conventional patch clamp amplifiers (EPC9/EPC10, HEKA Lamprecht, Germany).

Calcium imaging:

Primary cultured microglia were incubated with Fluo-4/AM (5 µM Fluo-4/AM, 0.1 % DMSO, 0.02 % w/v pluronic F-127) in HEPES buffer for 40 min. Before recording, cells were washed 10 – 15 min in HEPES buffer. Fluorescence signals were recorded at excitation and emission wavelengths of 488 nm and 510 nm, respectively, using a conventional polychromator (LPS-150, Till Photonics, Gräfelfing, Germany) and a camera (Sensicam, Photonics, Pittsfield MS, USA) attached to the microscope using water emerged 20x objectives (Olympus ,Shinjuku, Japan). During recording, cells were superfused with HEPES (3 - 4 mL/ min) buffer. Images were taken with a frequency of 2 frames/min and an exposure time of 50 ms.

Recording of intrinsic optical signals:

The intrinsic optical signal (IOS) was measured as light transmission via a camera attached to the microscope. Images were taken once per second. For analysis of ∆IOS we averaged the first 30 images of baseline recordings and subtracted them from all other images. We therefore normalized the IOS to illustrate changes in transmitted light in the recorded brain slices.

Induction of cortical spreading depression:

To induce cortical spreading depression in brain slices we placed an injection pipette (4 - 6 MΩ resistance) into the slice (20 – 50 µm deep) in layer 2 - 3 of the cortex and KCl was ejected in 3 – 5 pulses (100 ms, 40 psi) from micropipette containing 3M KCl. Field and patch electrodes were placed at least 350 µm apart to avoid diffusion artifacts.

Statistical analysis:

We used student's t-test to perform statistical analysis to compare the means of two groups. Significance was defined as * $p < 0.05$; ** $p < 0.01$; *** $p < 0.001$. Error bars are given as the standard error of the mean. For identification of significant outliers we used Grubb's outlier test.

Results

Microglial membrane currents evoked by cortical spreading depression

We employed a classical experimental paradigm to initiate cortical spreading depression in layer 2 - 3 of the cortex by ejecting 5 pulses (100 ms) of 3M KCl solution from a micropipette (Peters *et al.*, 2003). Simultaneously we recorded membrane currents from a microglial cell and the local field potential at least 500 µm away from the ejection electrode. The membrane potential of the microglial cell was clamped from -20 mV to a series of de- and hyperpolarizing values ranging from -140 mV to 60 mV with 20 mV increment and 100 ms duration to obtain current voltage curves with a frequency of 5 s (for stimulation protocol see Figure 1 A). Simultaneously we recorded the intrinsic optical signal (IOS) with an 4x objective (Olympus) in a 100 μm^2 area around the patch-pipette and field electrode (Figure 1 A, upper left). The ejection of potassium from the pipette triggered an IOS propagating with 46.6 ± 5.6 µm/sec (n = 7, Figure 1 A, 1 - 4). When IOS reached the field potential electrode, we recorded a negative DC potential shift. Simultaneously we recorded an inward rectifying increase in membrane conductance in the microglial cell (Figure 1 A, upper right part). The current activated rapidly and showed a voltage dependent inactivation increasing with hyperpolarization (Figure 1 B, upper part). Inward membrane current density increased by 2.5 ± 0.3 pA/pF at -140 mV membrane potential, but only 0.3 ± 0.1 pA/pF at 60 mV (n = 14). The reversal potential was at -11.6 ± 8.6 mV (n = 13) (Figure 1 B, lower part). In Figure 1 C ∆IOS images are given to four different time points of the recordings to

illustrate the propagation of the spreading depression. Microglial membrane currents and negative DC potential shifts returned to baseline within a few minutes whereas the IOS increase did not recover that quickly consistent with earlier reports (Peters et al., 2003; Zhou et al., 2013). Changes in the IOS are most likely due to cellular volume changes (Witte et al., 2001) and might need longer to recover compared to shifted ion concentrations leading to DC potential shifts and microglial membrane currents.

Potassium application mimics the CSD evoked currents

CSD is known to be accompanied by an increase in $[K^+]_o$ and the inward rectifying membrane currents of neonatal amoeboid microglia were increased by $[K^+]_o$ elevation (Cheung et al., 2009). We tested the effect of defined elevation in $[K^+]_o$ (10, 25 and 50 mM) on membrane currents of microglia in the adult cortex. Potassium mimicked the spreading depression induced inward rectifying currents (Figure 2 A). The kinetics of the currents induced by elevation in $[K^+]_o$ were similar as described above for CSD induced currents (shown in Figure 2 B for 50 mM $[K^+]_o$). An increase to 10 mM $[K^+]_o$ augmented inward membrane current density at -140 mV by 1 ± 0.1 pA/pF (n = 5), an increase to 25 mM by 2.3 ± 0.4 pA/pF (n = 15) and an increase to 50 mM by 5.7 ± 1.4 pA/pF (n =6) whereas spreading depression led to an increase by 2.5 ± 0.3 pA/pF (n = 14) as shown above (Figure 2 C). We therefore assume that an elevation of roughly 25 mM potassium occurred during CSD which is consistent with reported potassium concentrations (~ 30 mM) in the literature (Hablitz and Heinemann, 1989; Petzold et al., 2005). Both potassium (data not shown) and spreading depression induced inward currents were blocked in the presence of 1 mM barium indicating that both currents were due to K^+ inward rectifier (K_{ir}) activation. A detailed analysis on the effect of barium on microglial membrane properties and CSD induced currents in microglia is described in the following. We therefore hypothesize that cortical spreading depression induces an increase in $[K^+]_o$ which results in changes of microglial membrane currents.

CSD and CSD-induced microglial membrane currents are NMDA receptor dependent

The NMDA receptor is known to be crucial in the propagation of CSD (Lauritzen et al., 1988; Marrannes et al., 1988; Nellgard and Wieloch, 1992). We therefore investigated the influence of the NMDA receptor antagonist D-AP5 on the spreading depression induced DC potential shift and the microglial membrane currents (Figure 3 A). Spreading depression was induced 3 times with a wash-out time of 12 min (n = 7) or 20 min (n = 2), first as a control, then in the presence of 50 µM D-AP5 and then again after washout. The distance between the ejection pipette and the patch -and field pipette was at least 350 µm. The microglial inward current density at -140 mV membrane potential was decreased in the presence of D-AP5 from the control value of 3 ± 0.5 to 0.65 ± 0.2 pA/pF (n = 9, *** p = 0.0007, Figure 3 B, upper part) whereas the negative DC potential shift was inhibited from -4.4 ± -0.7 down to -0.5 ± 0.1 mV (n = 9, *** p = 0.0001, Figure 3 B, lower part). To analyze the recovery after D-AP5 application we normalized the measured amplitudes (DC potential shift and microglial current responses at -140 mV) of the second and third induced CSD to the first one. Microglial membrane currents decreased to 21.7 ± 4.8 % and recovered to 40.6 ± 5.6 % (n = 9, * p = 0.024).whereas the DC potential shifts decreased to 14 ± 5.2 % and recovered to 47.3 ± 10.9 % (n = 9, * p = 0.014). We conclude that cortical spreading depression and the resulting potassium currents in microglial cells depend on NMDA receptors activity.

CSD induced microglial membrane currents are modulated by CNQX

Even though AMPA/kainate receptors play a minor role in spreading depression (Lauritzen and Hansen, 1992; Nellgard and Wieloch, 1992) we investigated whether blockade of AMPA/kainate receptors influence CSD and CSD induced membrane currents. We recorded membrane currents from microglial cells, measured the DC potential and induced CSD. The AMPA/kainate receptor antagonist CNQX (10 µM) was applied 2 min prior CSD induction and wash-in was stopped 30 s afterwards. We compared DC potential shifts (-5.1 ± 0.4 to -4.4 ± 0.7 mV, n = 10 vs 9, p = 0.39,) and microglial inward membrane current densities (1.4 ± 0.3 to -2.5 ± 0.3 pA/pF, n = 10 vs 14, * p = 0.02, at -140 mV) to the control data. Whereas the DC potential shift was not altered, the microglial membrane currents were significantly decreased. We conclude that AMPA/kainate receptors in the acute brain slice are involved in the mechanism leading to CSD induced potassium currents in microglia.

NMDA mimics the CSD induced changes in microglial membrane currents

Next we investigated whether NMDA (100 µM) bath application itself results in microglial membrane currents in acute mouse brain slices. We employed the whole-cell patch-clamp technique as we described above. In addition we placed a field electrode close to the patched microglial cell (~50 - 150

µm) and recorded the IOS in the given field of view (n = 19, magnesium-free ACSF). When clamped at -20 mV NMDA did not lead to a change in membrane currents. At more negative potentials we recorded a similar membrane current increase as observed with elevation of $[K^+]_o$ or after initiation of CSD induced inward rectifying membrane currents in the patched microglial cells (Figure 4 A, upper part). The microglial membrane current response was accompanied by a simultaneous negative DC potential shift and an increase in IOS (Figure 4 A, lower part). The kinetics of NMDA induced current showed a fast activation and inactivation at low membrane potentials similar to the currents recorded during spreading depression and elevation of $[K^+]_o$ (Figure 4 B, left part). The amplitudes of the NMDA induced currents and the current voltage relationships were influenced by extracellular magnesium as shown in Figure 4 B (right part). In magnesium-free ACSF, amplitudes were significantly higher at negative membrane potentials with the largest differences at -140 mV with average inward current densities of 1.8 ± 0.2 pA/pF (n = 49) in magnesium-free ACSF and 0.79 ± 0.16 pA/pF (n = 19, ** p = 0.0046) in standard ACSF. The reversal potential of the NMDA induced current was at -23 ± 3 mV (n = 45) in magnesium-free ACSF. Upon application of D-AP5 (50 µM) the NMDA induced currents in microglia were completely blocked (Figure 4 C, n = 15). To confirm that all cells were viable we used ATP (1 mM) as a positive control which always elicited a profound conductance increase as it was described by Boucsein et al. (2003).

NMDA and CSD evoked currents in microglia are partially blocked by barium

We assume that NMDA increases the K_{ir} channel activity in microglia and we therefore tested the impact of Ba^{2+} (1 mM) as a well-known blocker of K_{ir} channels (Hibino et al., 2010). First we analyzed the effect of 1 mM Ba^{2+} on the membrane properties of microglial cells. The cells were clamped at -20 mV and voltage steps from -170 to 60 mV with 10 mV increments were given for 50 ms each. Resulting current patterns are shown in Figure 5 A (left part) for control and barium application (average of 9 cells each). Membrane currents were mainly reduced at negative membrane potentials down to 56.6 ± 4.9 % at -140 mV. The reversal potential of the subtracted current was close to the potassium equilibrium potential confirming baseline K_{ir} channel activity in adult cortical ramified microglia of acute brain slices (Figure 5 A, right part). We investigated whether the NMDA induced inward rectifying currents shown above are mediated by K_{ir} channels. We therefore applied NMDA in the presence of $BaCl_2$. NMDA did only induce a very small increase of inward membrane currents at potentials negative to -60 mV (0.18 ± 0.06 pA/pF at -140 mV, n = 9). Instead we observed an increase in outward currents at positive potentials (0.6 ± 0.09 pA/pF, n = 9; Figure 5 B, upper part). The current voltage curve of this current component shown in the lower part of Figure 5 B had a reversal potential of about -50 mV. The negative DC potential shift and the increased IOS upon NMDA application was still observed although the amplitude of the negative DC potential shift was reduced by half (-3.1 ± 0.2 mV, n = 19, to -1.4 ± 0.34 mV 3.1 ± 0.2, n = 9, *** p=0.0001). We conclude that the NMDA evoked inward rectifying current is mediated by K_{ir} and a non-K_{ir} mediated outward current is unmasked by Ba^{2+} which is similar to currents described by (Eyo et al., 2014). To study the effect of Ba^{2+} on CSD and CSD induced currents we repeated the experiments shown above (Figure 1) in the presence of 1 mM barium. Again inward rectifying membrane currents were blocked and a small outward current was unmasked in 6 out of 13 recordings, shown in Figure 5 C, with maximum amplitudes of 0.6 ± 0.2 pA/pF at 60 mV voltage steps. The DC potential however did not change significantly as compared to controls (-3.6 ± 0.4 to -4.4 ± 0.7 mV, n = 13 vs 9, p = 0.29).

CSD induced microglial membrane currents are inhibited by K_{ir} antagonists

Since barium is a rather unspecific K^+ channel blocker with known side-effects we employed more specific K_{ir} antagonists. So far it has been shown that cultured microglia mainly display K_{ir}2.1 currents which are effectively blocked by ML133 (Lam and Schlichter, 2015). It is however not known which inward rectifiers are expressed in microglia *in situ* or *in vivo.* We therefore first confirmed the results by Lam and Schlichter by applying our batch of ML133 (20 µM) to cultured neonatal microglia. We were able to confirm that ML133 is an effective K_{ir} blocker *in vitro* inhibiting 48 ± 7 % (Figure 6 A, n = 8) of membrane currents at -140 mV membrane potentials. We then applied ML133 (20 µM) while recording membrane currents from microglial cells in slices. We did only observe a 12 % inhibition of baseline inward currents at -140 mV (n = 6). Subsequently we tested the effect of ML133 (5 min preincubation) on the CSD induced currents. The CSD induced inward currents were 1.1 ± 0.2 pA/pF (n = 6) and thus smaller than control currents which were 2.5 pA/pF (see above). Thus the currents were reduced, but not completely blocked. We therefore used a cocktail of blockers directed against various K_{ir} subtypes (Glibenclamide (100 µM, K_{ir}6 family), ML133 (20 µM, K_{ir}2.1), Nortriptyline (K_{ir}4.1), Tertiapin-Q (200 nM, K_{ir}3.1 and Kir3.4) and VU590 (10 µM, K_{ir}1.1 and 7.1)) in a second set of experiments. In cultured microglial cells the whole cocktail of antagonists inhibited 57 ± 8 % of membrane currents (Figure 6 B,

n = 8). This inhibition was not significantly different when compared to ML133 alone (p = 0.41) confirming that K_{ir}2.1 is the most dominant potassium inward rectifier in cultured microglia.
We then tested this cocktail on microglia *in situ* (Figure 6 C). Only 14 % (5.2 ± 1.5 pA, n = 11, Figure 6 D) of the baseline currents at -140 mV were blocked which was significantly less compared to a 43 % (29.6 ± 7.5 pA, n 11 vs 9, ** p = 0.0024) inhibition by barium (Figure 5 A). We then compared the CSD induced currents in the presence of the K_{ir} antagonists to the control data shown above (Figure 1). The CSD induced inward current -140 mV was 1 ± 0.2 pA/pF (n = 14 vs 11, ** p = 0.0019, Figure 6 E) thus not significantly different to the value in the presence of ML133 alone. We excluded one recording which was a significant outlier (** p < 0.01, Grubb's outlier test) showing no baseline inhibition by K_{ir} antagonists and a profound CSD induced inward current of 5.5 pA/pF at a -140 mV membrane potential suggesting heterogeneity of K_{ir} activity of microglia *in situ.* We conclude that the dominant CSD induced current component is mediated by K_{ir}2.1, but that there is an additional component which is sensitive to barium, but not blocked by the currently available antagonists of K_{ir}.

NMDA induced inward currents are not influenced by the purinergic receptor blocker RB2

It was recently reported that neuronal NMDA receptor activation can trigger the activation of microglial purinergic receptors leading to process motility in the microglial cells which are inhibited by the purinergic antagonist Reactive Blue 2 (RB2) (Dissing-Olesen et al., 2014; Eyo et al., 2014). We therefore tested the effect of RB2 on the NMDA induced activation of K_{ir}. Microglial were patched and magnesium-free ACSF was used. As shown in Figure 7 A, K_{ir} channel activity was still observed in the presence of RB2 (100 µM).The current voltage relationship was not significantly affected. Neither inward current density at -140 mV membrane potential nor at 60 mV were significantly affected (2.25 ± 0.7 pA/pF for -140 mV, 0.2 ± 0.06 pA/pF for 60 mV, n = 17, Figure 7 B). We conclude that NMDA induced inward rectifying potassium currents are independent of P2Y receptor related purinergic signaling.

Adult cultured microglia do not respond to NMDA exposure

It was reported that neonatal microglial express functional NMDA receptors *in vitro* (Kaindl et al., 2012). We tested for the presence of functional NMDA receptors in microglial cultured from adult tissue by using the whole-cell patch-clamp technique and calcium imaging. We recorded membrane currents with a similar protocol as used for the *in situ* microglia and applied NMDA (100 µM) and ATP (1 mM) as a positive control. We did never observe any response to exposure of NMDA (n = 23, Figure 8 A) while ATP always triggered an increase in membrane currents as previously described (Walz et al., 1993). We also performed calcium imaging with Fluo-4 loaded adult microglia *in vitro* with the same wash-in protocol. In total we analyzed 10 coverslips with a sum of 207 cells (additional 100 cells displayed spontaneous activity and were excluded due to possible false positive results). We did not record any calcium elevations during NMDA applications or buffer controls (data not shown). Although nearly all cells responded to ATP application (91.3 ± 3.3 %, n = 10). Example traces are shown in Figure **8** B. We therefore conclude that the cells were viable and do not respond to NMDA exposure neither by current influx nor by intracellular increase of calcium levels.

Discussion

We demonstrate that in acute cortical mouse brain slices CSD induced an increase in the K^+ conductance of microglial cells. This increase in K^+ conductance can be mimicked by bath application of NMDA and an increase in extracellular $[K^+]$ and is blocked by the NMDA receptor antagonist D-AP5. It is well established that the NMDA receptor is crucial for initiation and propagation of CSD (Marrannes et al., 1988; Lauritzen and Hansen, 1992). There is, however, no evidence for the expression of functional NMDA receptors by microglial cells *in situ*. There are reports on functional NMDA receptor expression *in vitro*: (Hirayama and Kuriyama, 2001) showed that MK-801 (a well known blocker for NMDA receptors) is cytotoxic to microglial cells *in vitro* suggesting a presence of NMDA receptors on microglia and (Kaindl et al., 2012) showed responses to NMDA in neonatal microglial cells *in vitro* by using calcium imaging and patch-clamp. Two independent studies *in situ* described a neuron-microglial crosstalk involving neuronal NMDA receptors and microglial purinergic receptors without any evidence for functional microglial NMDA receptors on microglia (Dissing-Olesen et al., 2014; Eyo et al., 2014). We could confirm this by demonstrating that microglia isolated from adult mice do not respond with a membrane conductance increase or a calcium elevation upon application of NMDA. We thus assume that neuronal NMDA receptor activation during CSD leads to an increase in extracellular $[K^+]$ which results in the activation of inward rectifying currents in microglia. Macroglial NMDA receptors of astrocytes (Lalo et al., 2006) and oligodendrocytes (Karadottir et al., 2005) might play an additional role. Besides the involvement of NMDA receptors we investigated whether AMPA/kainate receptors are involved and found that CSD induced microglial K_{ir} currents, but

not DC potential shifts, are influenced by CNQX, an AMPA/kaiante receptor antagonist. Although it is believed that within the class of ionotropic glutamate receptors only NMDA receptors play a crucial role for CSD (Lauritzen and Hansen, 1992; Nellgard and Wieloch, 1992) there is evidence that AMPA receptors have at least regulatory effects on CSD (Kertesz et al., 2004; Holland et al., 2010). Indeed, we could block the microglial response to CSD and NMDA application by the K^+ channel blocker Ba^{2+} confirming that the microglial response is mediated by the activation of K^+ channels. This Ba^{2+} blockade unmasked a small outward current response with a current voltage relationship similar to a response to ATP (Boucsein et al., 2003) and thus confirming the observation by Eyo et al. (2014) that bath application of NMDA leads to ATP responses in hippocampal microglia. In their study they recorded currents only at a membrane potential of -20 mV and could thus not record the activation of the inward rectifier as we observed in our study. It is however interesting that they observed such currents without barium which might be the result of regional differences between cortical and hippocampal microglia. Moreover, we found that the purinergic receptor blocker RB2 did not block the NMDA induced K_{ir} current indicating that neuronal NMDA receptor activation leads to two distinct events, namely the CSD induced K_{ir} current activation reported in this study and the NMDA-ATP crosstalk reported by Dissing-Olesen et al. (2014) and Eyo et al. (2014). We also used specific antagonists for K_{ir} resulting in similar effects on baseline currents and CSD induced currents. It has been shown by Lam and Schlichter (2015) that K_{ir}2.1 is the dominant inward rectifyier K^+ channel *in vitro* which we could confirm employing the antagonist ML133. This antagonist had, however, only a small effect on the resting currents in microglia *in situ*. So far it is not known which channels are responsible for K_{ir} currents in microglia *in situ* and *in vivo*. We therefore used a cocktail of all subtype-specific K_{ir} antagonists which are currently available (Glibenclamide (K_{ir}6 family), ML133 (K_{ir}2.1), Nortriptyline (K_{ir}4.1), Tertiapin-Q (K_{ir}3.1 and K_{ir}3.4) and VU590 (K_{ir}1.1 and 7.1) which was, however, not more effective. Both ML133 and the cocktail blocked about 60 % of the CSD induced current. This indicates that a significant fraction of the current is mediated by K_{ir}2.1, but there is still a (barium-sensitive) current component which is not sensitive to the so far known K_{ir} antagonists. We also noted that the reversal potential of microglial currents blocked by these antagonists was not at the potassium equilibrium potential like we showed for the barium sensitive current.

Elevation in extracellular $[K^+]$ occurs in physiology and pathology while only under pathologic conditions extracellular $[K^+]$ exceeds 10 mM. Thus an extracellular $[K^+]$ increase has been considered as an activation signal for microglia. A $GABA_B$ receptors mediated increase in extracellular $[K^+]$ triggers macrophage inflammatory protein-1alpha release in amoeboid microglia of young mouse brain slices of the corpus callosum has been shown by Cheung et al. (2009). Activity of K_{ir} modulates ATP induced calcium signaling (Franchini et al., 2004) and blockade of K_{ir} reduces ATP induced chemotaxis and induces microglial proliferation *in vitro* (Lam and Schlichter, 2015). Thus the activation of K_{ir} induced by CSD may have an impact on microglial functions.

So far the role of microglia in initiation, propagation and recovery of CSD is poorly understood. There is, however, evidence that CSD has an impact on microglia. Hours after initiation of potassium induced spreading depression microglial cells upregulate markers of activation by showing an increased expression of MHC-II (Gehrmann et al., 1993) and IL-1ß (Jander et al., 2001). Spreading depression induces microglial migration and motility and the authors speculate that this response might influence the electrical activity of the surrounding tissue leading to higher susceptibility to CSD (Grinberg et al., 2011). Recently it was even suggested that microglial cytokine release is necessary for the initiation of spreading depression (Pusic et al., 2014). In conclusion, we show that microglial cells sense the CSD by activation of K_{ir} which might in turn modulate microglial behavior. The possible significance of microglial cells sensing and responding to potassium elevations in CSD could be relevant in a pathological context. CSD was reported to be associated with stroke (Strong et al., 2002) and traumatic brain injury (Hartings et al., 2009). Additionally it is reported that the pathophysiology of migraine aura and epilepsy share certain features and that migraine aura can trigger epileptic seizures (Nye and Thadani, 2015). Thus sensing CSD induced potassium elevations in a pathologic context might be a signal to microglia and could result in functional consequences.

Figure legends:

Figure 1: Cortical spreading depression induced by ejection of 3M KCl from a micro- pipette results in inward rectifying membrane currents in microglial cells. A: The positions of patch pipette, field electrode and potassium ejection pipette are shown on the left. The region where the IOS was recorded is indicated by the square. Microglial membrane currents are shown in the upper part as a response to a series of 100 ms long de- and hyperpolarizing voltage steps ranging from -140 to 60 mV with 20 mV increment from a holding potential of -20 mV. This pattern was continuously applied every 5 s. Stimulation protocol and current responses at baseline (BL) and at the peak (4) are shown on the left side. Simultaneously the DC field potential (black trace) and changes in IOS (grey trace) are shown at the lower right. Dashed lines and numbers indicate the time points corresponding to the images shown in C. The time point of potassium ejection is marked by an arrow. B: Membrane currents induced by cortical spreading depression were obtained by subtracting the currents at the peak of the response (4) from currents recorded before CSD was elicited (BL). The resulting current voltage relationship is shown below. The reversal

potential was at about -30 mV. C: The ΔIOS after induction of CSD is shown at different time points (1-4). Scale bars are 200 µm.

Figure 2: Increase in extracellular $[K^+]$ elicits similar membrane currents as CSD. A: Similar as described in the legend to Fig. 1 we recorded membrane currents at a series of de- and hyperpolarizing membrane potential jumps during an increase of $[K^+]_o$ from 5 to 10 mM (upper trace) and 50 mM (lower trace). K^+ induced currents in microglia. B: Membrane current kinetics induced by an increase of $[K^+]_o$ to 50 mM were obtained by subtracting currents in the presence of 50 mM $[K^+]$ from currents recorded at normal $[K^+]_o$. C: Current voltage relationships of subtracted currents are shown for 10, 25 and 50 mM K^+ applications together with the average current response to CSD.

Figure 3: CSD and induced microglial currents are inhibited by D-AP5. A: Microglial membrane currents (upper traces) and DC potential (lower traces) were recorded as described in the legend to Figure 1, before (left), during (middle) and after (right) a 2 min application of 50 µM D-AP5. Arrows indicate the time points of potassium ejections for triggering CSD. B: Averaged current voltage relationships of the membrane currents (peak response minus baseline) induced by CSD are shown for each of the three recordings shown in A. In the lower part the change in DC potential shifts are shown for each experiment for all three applications.

Figure 4: NMDA induced inward rectifying currents in microglia accompanied by negative DC potential shifts and increased IOS. A: Example recording of microglial membrane currents, as described in the legend of Figure 1, (upper trace) during bath application of NMDA (100 µM). Field recording and the change in the IOS are shown below. B: NMDA induced membrane currents at the different membrane potentials were obtained by subtracting currents at the peak of the NMDA response from currents prior to NMDA application and are shown on the left. On the right, mean NMDA induced currents were plotted against the membrane potential in magnesium-free ACSF (black) and standard ACSF (grey). C: Example recording of NMDA application in the presence of D-AP5 (50 µM) which was applied 30 s before, after and during the NMDA application. ATP was applied at the end as a positive control.

Figure 5: NMDA and CSD induced currents are partially blocked by barium. Membrane current response, DC potential and IOS were recorded as described in the legend to Fig. 1.A: Influence of barium (1 mM) on microglial membrane properties are shown. Microglia were clamped at -20 mV and voltage steps ranging from -170 to 60 mV with 10 mV increment each 50 ms long were applied. Barium blocked inward rectifying membrane currents with a reversal potential close to the potassium equilibrium potential. B: NMDA was applied as indicated by bar in presence of barium (1 mM). For calculation of current voltage relationships, baseline currents were subtracted from currents at the peak of the response. NMDA induced currents were plotted against membrane potential in the graph below. Note that NMDA induced a small outward rectifying response in the presence of barium. C: CSD induced membrane currents in the presence of barium are shown. Again a small outward rectifying component was unmasked with a reversal potential close to -20 mV.

Figure 6: CSD induced membrane currents are inhibited by a cocktail of K_{ir} antagonists. Membrane current response, DC potential and IOS were recorded as described in the legend to Fig. 1. Representative recordings are shown for baseline inhibitions of ML133 (20 µM) (A) and Glibenclamide (100 µM) , ML133 (20 µM), Nortriptyline (100 µM), Tertiapin-Q (200 nM) and VU590 (10 µM) (B) in patched neonatal cultured microglia. C: Influence of K_{ir} antagonists on microglial baseline currents and CSD induced currents. Dashed line indicates a 2 min period of perfusion stop allowing the blockers to incubate. D: Average baseline, block by K_{ir} antagonists and the subtracted current are shown as current voltage relationships. Note that the reversal potential is ~ 30 mV. E: Average CSD induced membrane currents are shown for control conditions and antagonist applications as current voltage relationships displaying an inward current inhibition of ~1.5 pA/pF at -140 mV membrane potentials (** p = 0.0019).

Figure 7: NMDA induced currents are not influenced by the purinergic receptor blocker RB2. A: Membrane current response during application of NMDA in combination with RB2 (100 µM, 30 s before, during and after NMDA application). Mean current voltage relationships of the NMDA induced currents in control solution and in combination with RB2 and controls. All experiments were done in magnesium-free ACSF.

Figure 8: NMDA application does not induce membrane currents or increased intracellular calcium levels in adult cultured microglia. A: Membrane currents were measured as described in the legend to Figure 1. NMDA did not trigger any responses. B: Example Fluo-4 fluorescence changes are shown from 5 microglial cells. No calcium increase was detected during NMDA application. ATP was used as a positive control for patch-clamp recordings and calcium imaging.

References

Avignone E, Lepleux M, Angibaud J, Nagerl UV (2015) Altered morphological dynamics of activated microglia after induction of status epilepticus. Journal of neuroinflammation 12:202.

Boucsein C, Zacharias R, Farber K, Pavlovic S, Hanisch UK, Kettenmann H (2003) Purinergic receptors on microglial cells: functional expression in acute brain slices and modulation of microglial activation in vitro. The European journal of neuroscience 17:2267-2276.

Cheung G, Kann O, Kohsaka S, Faerber K, Kettenmann H (2009) GABAergic activities enhance macrophage inflammatory protein-1alpha release from microglia (brain macrophages) in postnatal mouse brain. J Physiol 587:753-768.

Dissing-Olesen L, LeDue JM, Rungta RL, Hefendehl JK, Choi HB, MacVicar BA (2014) Activation of neuronal NMDA receptors triggers transient ATP-mediated microglial process outgrowth. The Journal of neuroscience : the official journal of the Society for Neuroscience 34:10511-10527.

Dreier JP (2011) The role of spreading depression, spreading depolarization and spreading ischemia in neurological disease. Nature medicine 17:439-447.

Eyo UB, Peng J, Swiatkowski P, Mukherjee A, Bispo A, Wu LJ (2014) Neuronal hyperactivity recruits microglial processes via neuronal NMDA receptors and microglial P2Y12 receptors after status epilepticus. The Journal of neuroscience : the official journal of the Society for Neuroscience 34:10528-10540.

Franchini L, Levi G, Visentin S (2004) Inwardly rectifying K+ channels influence Ca2+ entry due to nucleotide receptor activation in microglia. Cell calcium 35:449-459.

Gehrmann J, Mies G, Bonnekoh P, Banati R, Iijima T, Kreutzberg GW, Hossmann KA (1993) Microglial reaction in the rat cerebral cortex induced by cortical spreading depression. Brain pathology 3:11-17.

Giulian D, Baker TJ (1986) Characterization of ameboid microglia isolated from developing mammalian brain. The Journal of neuroscience : the official journal of the Society for Neuroscience 6:2163-2178.
Grinberg YY, Milton JG, Kraig RP (2011) Spreading depression sends microglia on Levy flights. PloS one 6:e19294.
Hablitz JJ, Heinemann U (1989) Alterations in the microenvironment during spreading depression associated with epileptiform activity in the immature neocortex. Brain research Developmental brain research 46:243-252.
Hanisch UK, Kettenmann H (2007) Microglia: active sensor and versatile effector cells in the normal and pathologic brain. Nature neuroscience 10:1387-1394.
Hartings JA, Strong AJ, Fabricius M, Manning A, Bhatia R, Dreier JP, Mazzeo AT, Tortella FC, Bullock MR, Co-Operative Study of Brain Injury D (2009) Spreading depolarizations and late secondary insults after traumatic brain injury. Journal of neurotrauma 26:1857-1866.
Hibino H, Inanobe A, Furutani K, Murakami S, Findlay I, Kurachi Y (2010) Inwardly rectifying potassium channels: their structure, function, and physiological roles. Physiol Rev 90:291-366.
Hirayama M, Kuriyama M (2001) MK-801 is cytotoxic to microglia in vitro and its cytotoxicity is attenuated by glutamate, other excitotoxic agents and atropine. Possible presence of glutamate receptor and muscarinic receptor on microglia. Brain research 897:204-206.
Holland PR, Akerman S, Goadsby PJ (2010) Cortical spreading depression-associated cerebral blood flow changes induced by mechanical stimulation are modulated by AMPA and GABA receptors. Cephalalgia : an international journal of headache 30:519-527.
Jander S, Schroeter M, Peters O, Witte OW, Stoll G (2001) Cortical spreading depression induces proinflammatory cytokine gene expression in the rat brain. Journal of cerebral blood flow and metabolism : official journal of the International Society of Cerebral Blood Flow and Metabolism 21:218-225.
Kaindl AM, Degos V, Peineau S, Gouadon E, Chhor V, Loron G, Le Charpentier T, Josserand J, Ali C, Vivien D, Collingridge GL, Lombet A, Issa L, Rene F, Loeffler JP, Kavelaars A, Verney C, Mantz J, Gressens P (2012) Activation of microglial N-methyl-D-aspartate receptors triggers inflammation and neuronal cell death in the developing and mature brain. Ann Neurol 72:536-549.
Karadottir R, Cavelier P, Bergersen LH, Attwell D (2005) NMDA receptors are expressed in oligodendrocytes and activated in ischaemia. Nature 438:1162-1166.
Kertesz S, Kapus G, Levay G (2004) Interactions of allosteric modulators of AMPA/kainate receptors on spreading depression in the chicken retina. Brain research 1025:123-129.
Kettenmann H, Hanisch UK, Noda M, Verkhratsky A (2011) Physiology of microglia. Physiol Rev 91:461-553.
Lalo U, Pankratov Y, Kirchhoff F, North RA, Verkhratsky A (2006) NMDA receptors mediate neuron-to-glia signaling in mouse cortical astrocytes. The Journal of neuroscience : the official journal of the Society for Neuroscience 26:2673-2683.
Lam D, Schlichter LC (2015) Expression and contributions of the Kir2.1 inward-rectifier K(+) channel to proliferation, migration and chemotaxis of microglia in unstimulated and anti-inflammatory states. Front Cell Neurosci 9:185.
Lauritzen M (1992) Spreading depression and migraine. Pathol Biol (Paris) 40:332-337.
Lauritzen M, Hansen AJ (1992) The effect of glutamate receptor blockade on anoxic depolarization and cortical spreading depression. Journal of cerebral blood flow and metabolism : official journal of the International Society of Cerebral Blood Flow and Metabolism 12:223-229.
Lauritzen M, Rice ME, Okada Y, Nicholson C (1988) Quisqualate, kainate and NMDA can initiate spreading depression in the turtle cerebellum. Brain research 475:317-327.
Leão AAP (1944) Spreading depression of activity in the cerebral cortex. Journal of Neurophysiology 7:391-396.
Marrannes R, Willems R, De Prins E, Wauquier A (1988) Evidence for a role of the N-methyl-D-aspartate (NMDA) receptor in cortical spreading depression in the rat. Brain research 457:226-240.
Nellgard B, Wieloch T (1992) NMDA-receptor blockers but not NBQX, an AMPA-receptor antagonist, inhibit spreading depression in the rat brain. Acta physiologica Scandinavica 146:497-503.
Nimmerjahn A, Kirchhoff F, Helmchen F (2005) Resting microglial cells are highly dynamic surveillants of brain parenchyma in vivo. Science 308:1314-1318.
Nye BL, Thadani VM (2015) Migraine and epilepsy: review of the literature. Headache 55:359-380.
Peters O, Schipke CG, Hashimoto Y, Kettenmann H (2003) Different mechanisms promote astrocyte Ca2+ waves and spreading depression in the mouse neocortex. The Journal of neuroscience : the official journal of the Society for Neuroscience 23:9888-9896.
Petzold GC, Windmuller O, Haack S, Major S, Buchheim K, Megow D, Gabriel S, Lehmann TN, Drenckhahn C, Peters O, Meierkord H, Heinemann U, Dirnagl U, Dreier JP (2005) Increased extracellular K+ concentration reduces the efficacy of N-methyl-D-aspartate receptor antagonists to block spreading depression-like depolarizations and spreading ischemia. Stroke; a journal of cerebral circulation 36:1270-1277.
Pusic KM, Pusic AD, Kemme J, Kraig RP (2014) Spreading depression requires microglia and is decreased by their M2a polarization from environmental enrichment. Glia 62:1176-1194.
Scheffel J, Regen T, Van Rossum D, Seifert S, Ribes S, Nau R, Parsa R, Harris RA, Boddeke HW, Chuang HN, Pukrop T, Wessels JT, Jurgens T, Merkler D, Bruck W, Schnaars M, Simons M, Kettenmann H, Hanisch UK (2012) Toll-like receptor activation reveals developmental reorganization and unmasks responder subsets of microglia. Glia 60:1930-1943.
Strong AJ, Fabricius M, Boutelle MG, Hibbins SJ, Hopwood SE, Jones R, Parkin MC, Lauritzen M (2002) Spreading and synchronous depressions of cortical activity in acutely injured human brain. Stroke; a journal of cerebral circulation 33:2738-2743.
Walz W, Ilschner S, Ohlemeyer C, Banati R, Kettenmann H (1993) Extracellular ATP activates a cation conductance and a K+ conductance in cultured microglial cells from mouse brain. The Journal of neuroscience : the official journal of the Society for Neuroscience 13:4403-4411.
Witte OW, Niermann H, Holthoff K (2001) Cell swelling and ion redistribution assessed with intrinsic optical signals. Anais da Academia Brasileira de Ciencias 73:337-350.
Zhou N, Rungta RL, Malik A, Han H, Wu DC, MacVicar BA (2013) Regenerative glutamate release by presynaptic NMDA receptors contributes to spreading depression. Journal of cerebral blood flow and metabolism : official journal of the International Society of Cerebral Blood Flow and Metabolism 33:1582-1594.

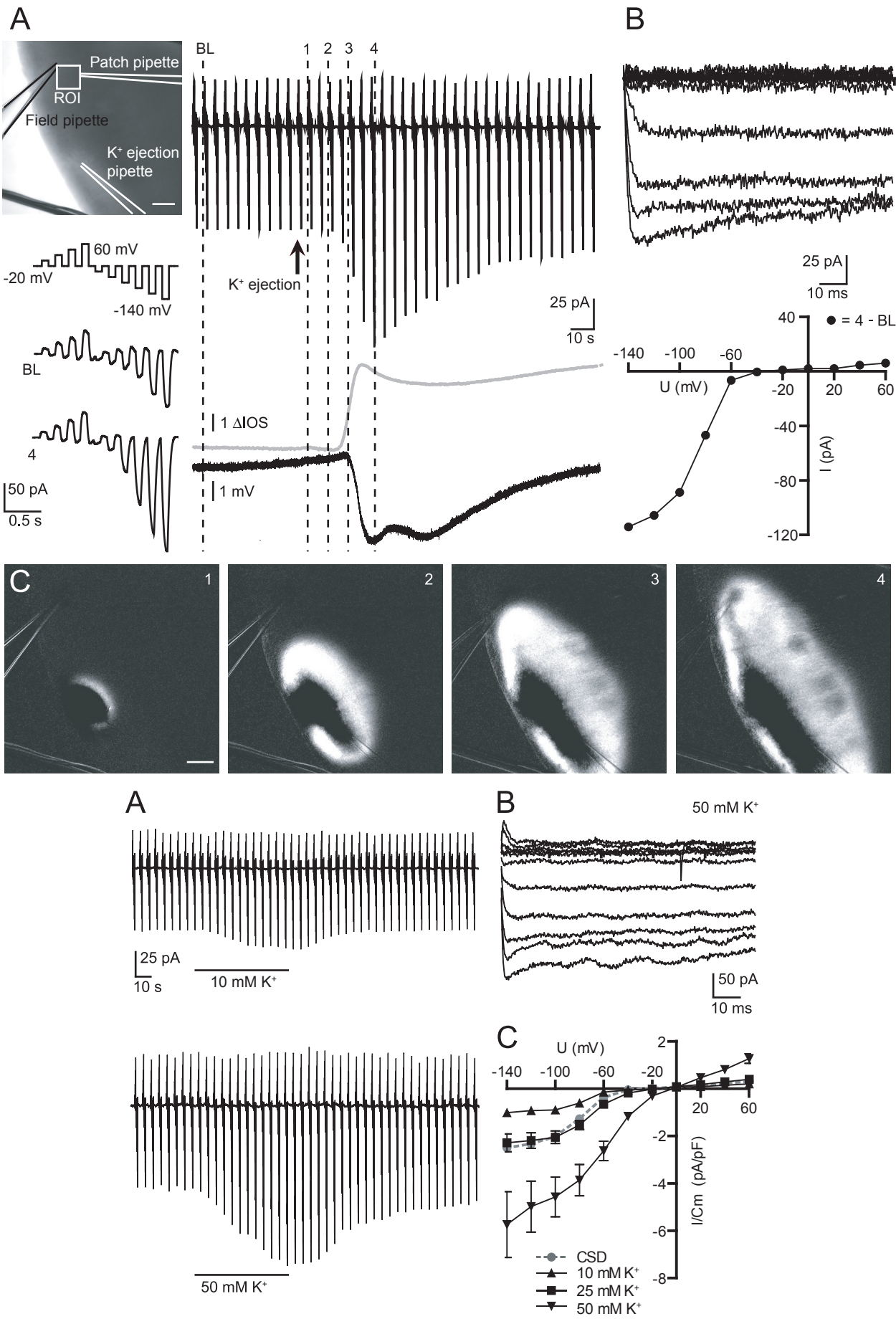
A
Patch pipette
ROI
Field pipette
K+ ejection pipette
BL
1
2
3
4
60 mV
-20 mV
-140 mV
K+ ejection
25 pA
10 s
BL
1 ΔIOS
4
50 pA
0.5 s
1 mV
B
25 pA
10 ms
40
● = 4 - BL
-140
-100
-60
U (mV)
-20
20
60
-40
-80
-120
I (pA)
C
1
2
3
4
A
25 pA
10 s
10 mM K+
50 mM K+
B
50 mM K+
50 pA
10 ms
C
U (mV)
-140
-100
-60
-20
20
60
2
-2
-4
-6
-8
I/Cm (pA/pF)
CSD
10 mM K+
25 mM K+
50 mM K+

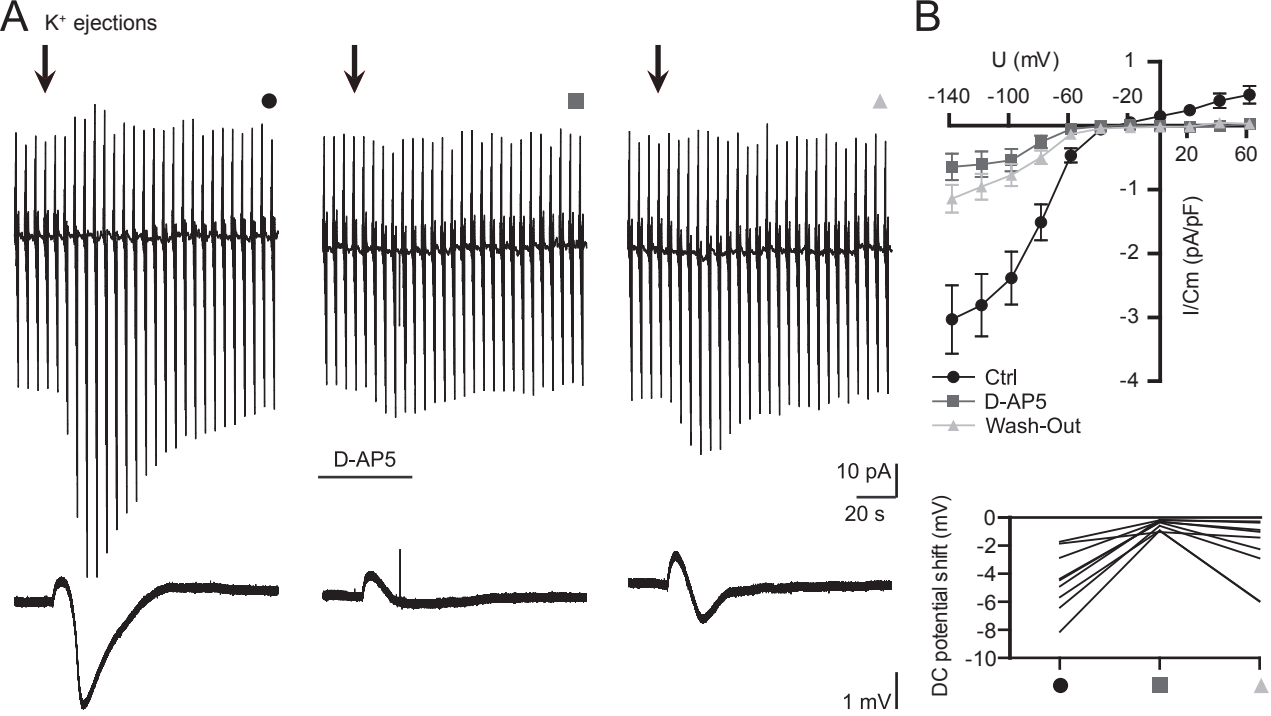
A
K+ ejections
D-AP5
10 pA
20 s
1 mV
B
U (mV)
-140 -100 -60 -20 1
20 60
-1 -2 -3 -4
I/Cm (pA/pF)
Ctrl
D-AP5
Wash-Out
DC potential shift (mV)
0 -2 -4 -6 -8 -10

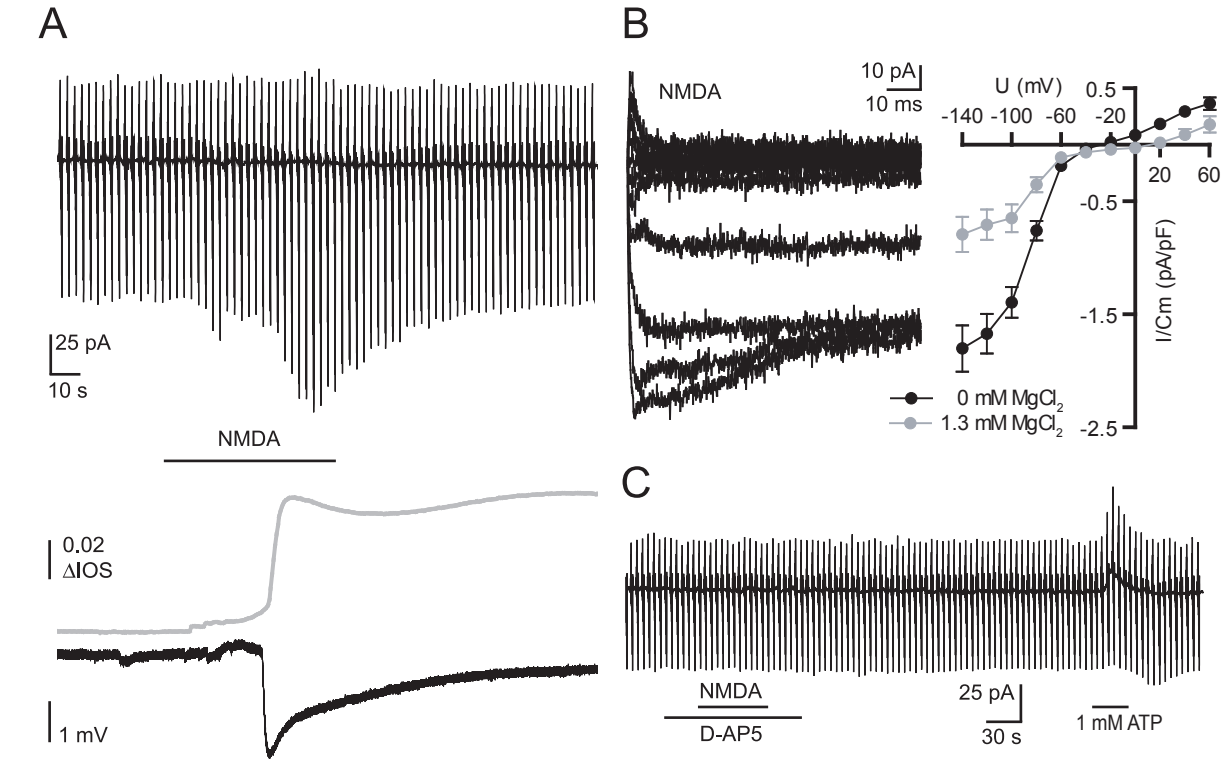
A
25 pA
10 s
NMDA
0.02
ΔIOS
1 mV
B
NMDA
10 pA
10 ms
U (mV)
-140 -100 -60 -20 0.5
20 60
-0.5 -1.5 -2.5
I/Cm (pA/pF)
0 mM MgCl2
1.3 mM MgCl2
C
NMDA
D-AP5
25 pA
30 s
1 mM ATP

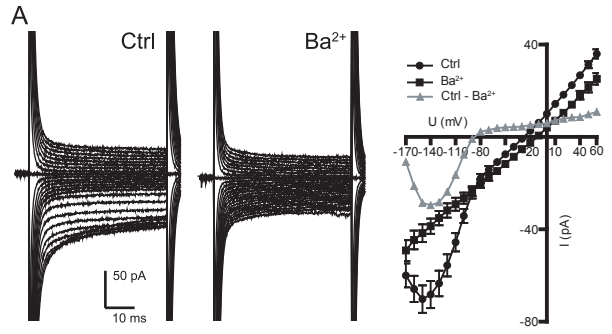
A
Ctrl
Ba2+
50 pA
10 ms
Ctrl
Ba2+
Ctrl - Ba2+
U (mV)
-170 -140 -110 -80 -20 10 40 60
40
-40
-80
I (pA)

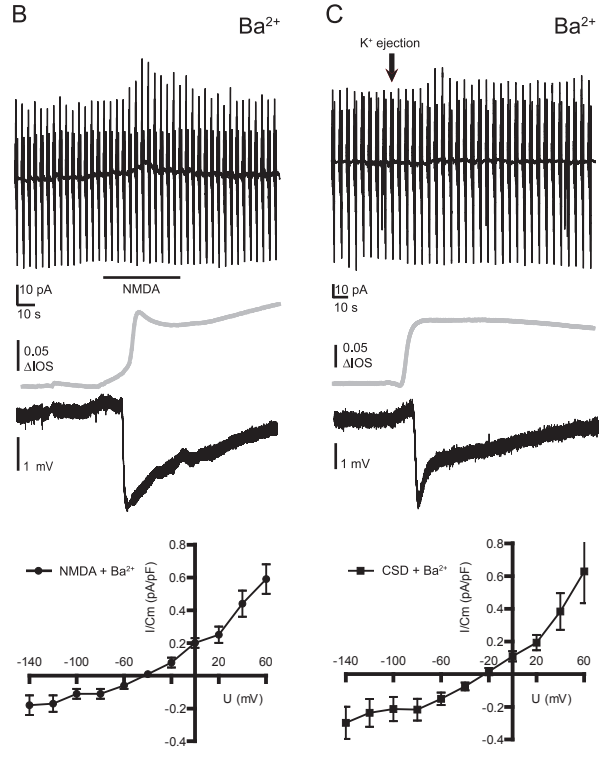
B
Ba2+
C
Ba2+
K+ ejection
10 pA
10 s
NMDA
0.05
ΔIOS
1 mV
NMDA + Ba2+
CSD + Ba2+
I/Cm (pA/pF)
U (mV)
0.8
0.6
0.4
0.2
-0.2
-0.4
-140 -100 -60 -20 20 60

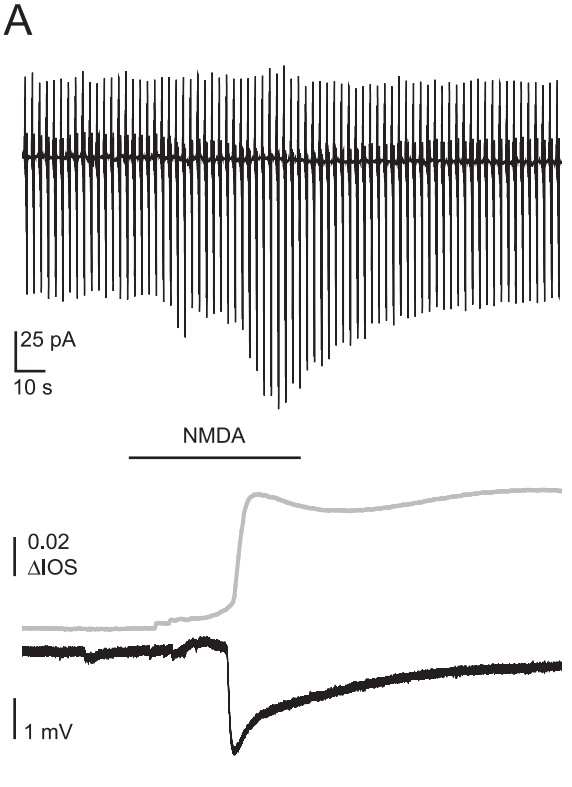
A
25 pA
10 s
NMDA
0.02
ΔIOS
1 mV

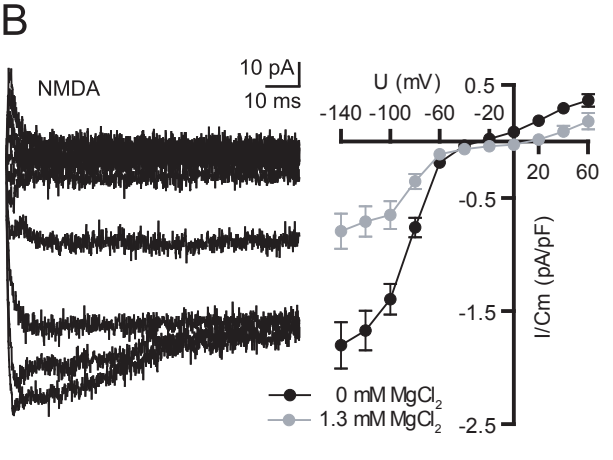
B
NMDA
10 pA
10 ms
U (mV)
-140 -100 -60 -20 20 60
0.5
-0.5
-1.5
-2.5
I/Cm (pA/pF)
0 mM MgCl2
1.3 mM MgCl2

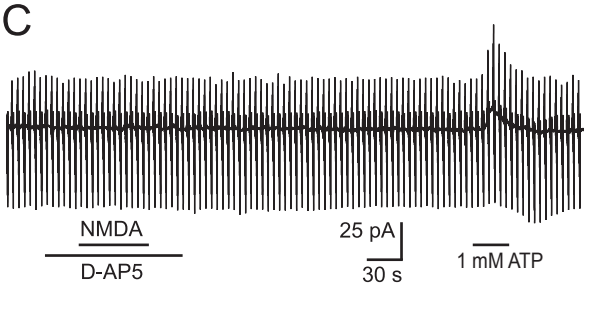
C
NMDA
D-AP5
25 pA
30 s
1 mM ATP

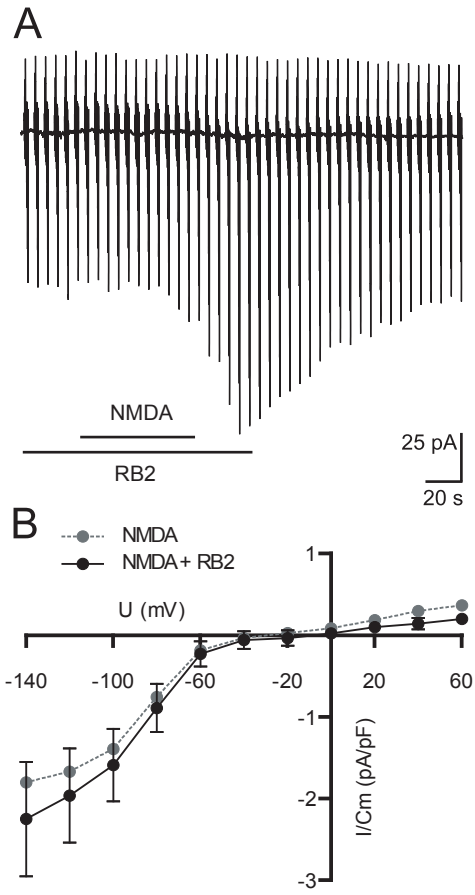
A
NMDA
RB2
25 pA
20 s
B
NMDA
NMDA+ RB2
U (mV)
-140
-100
-60
-20
20
60
1
-1
-2
-3
I/Cm (pA/pF)

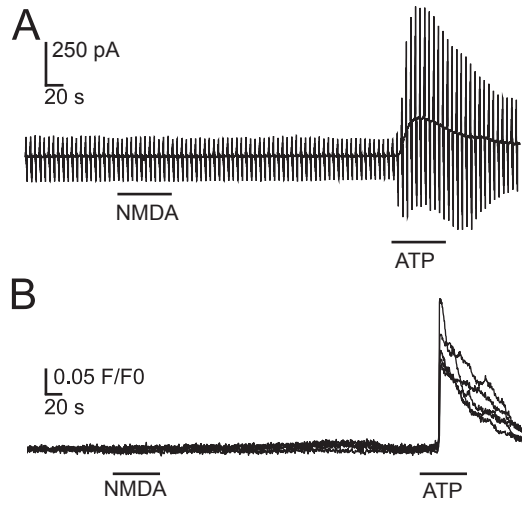
A
250 pA
20 s
NMDA
ATP
B
0.05 F/F0
20 s
NMDA
ATP

Grinberg YY, Milton JG, Kraig RP (2011) Spreading depression sends microglia on Lévy flights. PloS One 6:e19294. CrossRef Medline

Hablitz JJ, Heinemann U (1989) Alterations in the microenvironment during spreading depression associated with epileptiform activity in the immature neocortex. Brain Res Dev Brain Res 46:243–252. CrossRef Medline

Hanisch UK, Kettenmann H (2007) Microglia: active sensor and versatile effector cells in the normal and pathologic brain. Nat Neurosci 10:1387–1394. CrossRef Medline

Hartings JA, Strong AJ, Fabricius M, Manning A, Bhatia R, Dreier JP, Mazzeo AT, Tortella FC, Bullock MR; Co-Operative Study of Brain Injury Depolarizations (2009) Spreading depolarizations and late secondary insults after traumatic brain injury. J Neurotrauma 26:1857–1866. CrossRef Medline

Hibino H, Inanobe A, Furutani K, Murakami S, Findlay I, Kurachi Y (2010) Inwardly rectifying potassium channels: their structure, function, and physiological roles. Physiol Rev 90:291–366. CrossRef Medline

Hirayama M, Kuriyama M (2001) MK-801 is cytotoxic to microglia in vitro and its cytotoxicity is attenuated by glutamate, other excitotoxic agents and atropine: possible presence of glutamate receptor and muscarinic receptor on microglia. Brain Res 897:204–206. CrossRef Medline

Holland PR, Akerman S, Goadsby PJ (2010) Cortical spreading depression-associated cerebral blood flow changes induced by mechanical stimulation are modulated by AMPA and GABA receptors. Cephalalgia 30:519–527. CrossRef Medline

Jander S, Schroeter M, Peters O, Witte OW, Stoll G (2001) Cortical spreading depression induces proinflammatory cytokine gene expression in the rat brain. J Cereb Blood Flow Metab 21:218–225. CrossRef Medline

Kaindl AM, Degos V, Peineau S, Gouadon E, Chhor V, Loron G, Le Charpentier T, Josserand J, Ali C, Vivien D, Collingridge GL, Lombet A, Issa L, Rene F, Loeffler JP, Kavelaars A, Verney C, Mantz J, Gressens P (2012) Activation of microglial *N*-methyl-D-aspartate receptors triggers inflammation and neuronal cell death in the developing and mature brain. Ann Neurol 72:536–549. CrossRef Medline

Káradóttir R, Cavelier P, Bergersen LH, Attwell D (2005) NMDA receptors are expressed in oligodendrocytes and activated in ischaemia. Nature 438:1162–1166. CrossRef Medline

Kertész S, Kapus G, Lévay G (2004) Interactions of allosteric modulators of AMPA/kainate receptors on spreading depression in the chicken retina. Brain Res 1025:123–129. CrossRef Medline

Kettenmann H, Hanisch UK, Noda M, Verkhratsky A (2011) Physiology of microglia. Physiol Rev 91:461–553. CrossRef Medline

Lalo U, Pankratov Y, Kirchhoff F, North RA, Verkhratsky A (2006) NMDA receptors mediate neuron-to-glia signaling in mouse cortical astrocytes. J Neurosci 26:2673–2683. CrossRef Medline

Lam D, Schlichter LC (2015) Expression and contributions of the Kir2.1 inward-rectifier K(+) channel to proliferation, migration and chemotaxis of microglia in unstimulated and anti-inflammatory states. Front Cell Neurosci 9:185. CrossRef Medline

Lauritzen M (1992) Spreading depression and migraine. Pathol Biol 40:332–337. Medline

Lauritzen M, Hansen AJ (1992) The effect of glutamate receptor blockade on anoxic depolarization and cortical spreading depression. J Cereb Blood Flow Metab 12:223–229. CrossRef Medline

Lauritzen M, Rice ME, Okada Y, Nicholson C (1988) Quisqualate, kainate and NMDA can initiate spreading depression in the turtle cerebellum. Brain Res 475:317–327. CrossRef Medline

Leão AAP (1944) Spreading depression of activity in the cerebral cortex. J Neurophysiol 7:359–390.

Marrannes R, Willems R, De Prins E, Wauquier A (1988) Evidence for a role of the *N*-methyl-D-aspartate (NMDA) receptor in cortical spreading depression in the rat. Brain Res 457:226–240. CrossRef Medline

Murugan M, Sivakumar V, Lu J, Ling EA, Kaur C (2011) Expression of N-methyl D-aspartate receptor subunits in amoeboid microglia mediates production of nitric oxide via NF-κB signaling pathway and oligodendrocyte cell death in hypoxic postnatal rats. Glia 59:521–539.

Nellgård B, Wieloch T (1992) NMDA-receptor blockers but not NBQX, an AMPA-receptor antagonist, inhibit spreading depression in the rat brain. Acta Physiologica Scandinavica 146:497–503. CrossRef Medline

Nimmerjahn A, Kirchhoff F, Helmchen F (2005) Resting microglial cells are highly dynamic surveillants of brain parenchyma in vivo. Science 308:1314–1318. CrossRef Medline

Nye BL, Thadani VM (2015) Migraine and epilepsy: review of the literature. Headache 55:359–380. CrossRef Medline

Peters O, Schipke CG, Hashimoto Y, Kettenmann H (2003) Different mechanisms promote astrocyte Ca2+ waves and spreading depression in the mouse neocortex. J Neurosci 23:9888–9896. Medline

Petzold GC, Windmüller O, Haack S, Major S, Buchheim K, Megow D, Gabriel S, Lehmann TN, Drenckhahn C, Peters O, Meierkord H, Heinemann U, Dirnagl U, Dreier JP (2005) Increased extracellular K+ concentration reduces the efficacy of *N*-methyl-D-aspartate receptor antagonists to block spreading depression-like depolarizations and spreading ischemia. Stroke 36:1270–1277. CrossRef Medline

Pusic KM, Pusic AD, Kemme J, Kraig RP (2014) Spreading depression requires microglia and is decreased by their M2a polarization from environmental enrichment. Glia 62:1176–1194. CrossRef Medline

Sasmono RT, Williams E (2012) Generation and characterization of MacGreen mice, the Cfs1r-EGFP transgenic mice. Methods Mol Biol 844:157–176.

Scheffel J, Regen T, Van Rossum D, Seifert S, Ribes S, Nau R, Parsa R, Harris RA, Boddeke HW, Chuang HN, Pukrop T, Wessels JT, Jürgens T, Merkler D, Brück W, Schnaars M, Simons M, Kettenmann H, Hanisch UK (2012) Toll-like receptor activation reveals developmental reorganization and unmasks responder subsets of microglia. Glia 60:1930–1943. CrossRef Medline

Strong AJ, Fabricius M, Boutelle MG, Hibbins SJ, Hopwood SE, Jones R, Parkin MC, Lauritzen M (2002) Spreading and synchronous depressions of cortical activity in acutely injured human brain. Stroke 33:2738–2743. CrossRef Medline

Walz W, Ilschner S, Ohlemeyer C, Banati R, Kettenmann H (1993) Extracellular ATP activates a cation conductance and a K+ conductance in cultured microglial cells from mouse brain. J Neurosci 13:4403–4411. Medline

Witte OW, Niermann H, Holthoff K (2001) Cell swelling and ion redistribution assessed with intrinsic optical signals. Anais da Academia Brasileira de Ciencias 73:337–350. CrossRef Medline

Zhou N, Rungta RL, Malik A, Han H, Wu DC, MacVicar BA (2013) Regenerative glutamate release by presynaptic NMDA receptors contributes to spreading depression. J Cereb Blood Flow Metab 33:1582–1594. CrossRef Medline

A comparative morphological, electrophysiological and functional analysis of axon regeneration through peripheral nerve autografts genetically modified to overexpress BDNF, CNTF, GDNF, NGF, NT3 or VEGF.

Hoyng SA, De Winter F, Gnavi S, de Boer R, Boon LI, Korvers LM, Tannemaat MR, Malessy MJ, Verhaagen J.

https://doi.org/10.1016/j.expneurol.2014.08.002

A comparative morphological, electrophysiological and functional analysis of axon regeneration through peripheral nerve autografts genetically modified to overexpress BDNF, CNTF, GDNF, NGF, NT3 or VEGF.

Hoyng SA, De Winter F, Gnavi S, de Boer R, Boon LI, Korvers LM, Tannemaat MR, Malessy MJ, Verhaagen J.

https://doi.org/10.1016/j.expneurol.2014.08.002

A comparative morphological, electrophysiological and functional analysis of axon regeneration through peripheral nerve autografts genetically modified to overexpress BDNF, CNTF, GDNF, NGF, NT3 or VEGF.

Hoyng SA, De Winter F, Gnavi S, de Boer R, Boon LI, Korvers LM, Tannemaat MR, Malessy MJ, Verhaagen J.

https://doi.org/10.1016/j.expneurol.2014.08.002

A comparative morphological, electrophysiological and functional analysis of axon regeneration through peripheral nerve autografts genetically modified to overexpress BDNF, CNTF, GDNF, NGF, NT3 or VEGF.

Hoyng SA, De Winter F, Gnavi S, de Boer R, Boon LI, Korvers LM, Tannemaat MR, Malessy MJ, Verhaagen J.

https://doi.org/10.1016/j.expneurol.2014.08.002

A comparative morphological, electrophysiological and functional analysis of axon regeneration through peripheral nerve autografts genetically modified to overexpress BDNF, CNTF, GDNF, NGF, NT3 or VEGF.

Hoyng SA, De Winter F, Gnavi S, de Boer R, Boon LI, Korvers LM, Tannemaat MR, Malessy MJ, Verhaagen J.

https://doi.org/10.1016/j.expneurol.2014.08.002

A comparative morphological, electrophysiological and functional analysis of axon regeneration through peripheral nerve autografts genetically modified to overexpress BDNF, CNTF, GDNF, NGF, NT3 or VEGF.

Hoyng SA, De Winter F, Gnavi S, de Boer R, Boon LI, Korvers LM, Tannemaat MR, Malessy MJ, Verhaagen J.

https://doi.org/10.1016/j.expneurol.2014.08.002

A comparative morphological, electrophysiological and functional analysis of axon regeneration through peripheral nerve autografts genetically modified to overexpress BDNF, CNTF, GDNF, NGF, NT3 or VEGF.

Hoyng SA, De Winter F, Gnavi S, de Boer R, Boon LI, Korvers LM, Tannemaat MR, Malessy MJ, Verhaagen J.

https://doi.org/10.1016/j.expneurol.2014.08.002

A comparative morphological, electrophysiological and functional analysis of axon regeneration through peripheral nerve autografts genetically modified to overexpress BDNF, CNTF, GDNF, NGF, NT3 or VEGF.

Hoyng SA, De Winter F, Gnavi S, de Boer R, Boon LI, Korvers LM, Tannemaat MR, Malessy MJ, Verhaagen J.

https://doi.org/10.1016/j.expneurol.2014.08.002

A comparative morphological, electrophysiological and functional analysis of axon regeneration through peripheral nerve autografts genetically modified to overexpress BDNF, CNTF, GDNF, NGF, NT3 or VEGF.

Hoyng SA, De Winter F, Gnavi S, de Boer R, Boon LI, Korvers LM, Tannemaat MR, Malessy MJ, Verhaagen J.

https://doi.org/10.1016/j.expneurol.2014.08.002

A comparative morphological, electrophysiological and functional analysis of axon regeneration through peripheral nerve autografts genetically modified to overexpress BDNF, CNTF, GDNF, NGF, NT3 or VEGF.

Hoyng SA, De Winter F, Gnavi S, de Boer R, Boon LI, Korvers LM, Tannemaat MR, Malessy MJ, Verhaagen J.

https://doi.org/10.1016/j.expneurol.2014.08.002

A comparative morphological, electrophysiological and functional analysis of axon regeneration through peripheral nerve autografts genetically modified to overexpress BDNF, CNTF, GDNF, NGF, NT3 or VEGF.

Hoyng SA, De Winter F, Gnavi S, de Boer R, Boon LI, Korvers LM, Tannemaat MR, Malessy MJ, Verhaagen J.

https://doi.org/10.1016/j.expneurol.2014.08.002

A comparative morphological, electrophysiological and functional analysis of axon regeneration through peripheral nerve autografts genetically modified to overexpress BDNF, CNTF, GDNF, NGF, NT3 or VEGF.

Hoyng SA, De Winter F, Gnavi S, de Boer R, Boon LI, Korvers LM, Tannemaat MR, Malessy MJ, Verhaagen J.

https://doi.org/10.1016/j.expneurol.2014.08.002

A comparative morphological, electrophysiological and functional analysis of axon regeneration through peripheral nerve autografts genetically modified to overexpress BDNF, CNTF, GDNF, NGF, NT3 or VEGF.

Hoyng SA, De Winter F, Gnavi S, de Boer R, Boon LI, Korvers LM, Tannemaat MR, Malessy MJ, Verhaagen J.

https://doi.org/10.1016/j.expneurol.2014.08.002

A comparative morphological, electrophysiological and functional analysis of axon regeneration through peripheral nerve autografts genetically modified to overexpress BDNF, CNTF, GDNF, NGF, NT3 or VEGF.

Hoyng SA, De Winter F, Gnavi S, de Boer R, Boon LI, Korvers LM, Tannemaat MR, Malessy MJ, Verhaagen J.

https://doi.org/10.1016/j.expneurol.2014.08.002

A comparative morphological, electrophysiological and functional analysis of axon regeneration through peripheral nerve autografts genetically modified to overexpress BDNF, CNTF, GDNF, NGF, NT3 or VEGF.

Hoyng SA, De Winter F, Gnavi S, de Boer R, Boon LI, Korvers LM, Tannemaat MR, Malessy MJ, Verhaagen J.

https://doi.org/10.1016/j.expneurol.2014.08.002

A comparative morphological, electrophysiological and functional analysis of axon regeneration through peripheral nerve autografts genetically modified to overexpress BDNF, CNTF, GDNF, NGF, NT3 or VEGF.

Hoyng SA, De Winter F, Gnavi S, de Boer R, Boon LI, Korvers LM, Tannemaat MR, Malessy MJ, Verhaagen J.

https://doi.org/10.1016/j.expneurol.2014.08.002

My curriculum vitae does not appear in the electronic version of my paper for reasons of data protection.

My curriculum vitae does not appear in the electronic version of my paper for reasons of data protection.

5 Complete list of publications

Publications

Hoyng SA, De Winter F, Gnavi S, de Boer R, Boon LI, **Korvers LM**, Tannemaat MR, Malessy MJ, Verhaagen J.
A comparative morphological, electrophysiological and functional analysis of axon regeneration through peripheral nerve autografts genetically modified to overexpress BDNF, CNTF, GDNF, NGF, NT3 or VEGF.
Exp Neurol. 2014 Nov; 261:578-93. doi: 10.1016/j.expneurol.2014.08.002. Epub 2014 Aug 12.
Impact factor 2014: 4.696

Wendt S, Wogram E, **Korvers L**, Kettenmann H.
Experimental Cortical Spreading Depression Induces NMDA Receptor Dependent Potassium Currents in Microglia.
J Neurosci. 2016 Jun 8;36(23):6165-74. doi: 10.1523/JNEUROSCI.4498-15.2016.
Impact factor 2014/2015: 6.344

Laura Korvers, Amanda de Andrade Costa, Martin Mersch, Vitali Matyash, Helmut Kettenmann and Marcus Semtner
Spontaneous Ca^{2+} transients in mouse microglia
Cell Calcium. 2016 Sep 22.; S0143-4160(16)30106-3. doi: 10.1016/j.ceca.2016.09.004.
Impact factor 2014/2015: 3.513

Poster presentations

Spontaneous calcium elevations in microglia **L. Korvers**, V. Matyash, M. Semtner, H. Kettenmann
XII European Meeting on Glial Cells in Health and Disease Bilbao, Spain 14.07.15 - 18.07.15

Spontaneous calcium elevations in microglia

L. Korvers, V. Matyash, M. Semtner, H. Kettenmann

SFB TRR 43 MGK retreat Berlin, Germany 01.10.2015

Spontaneous calcium elevations in microglia

L. Korvers, V. Matyash, M. Semtner, H. Kettenmann

MDC/FMP PhD retreat Bad Saarow, Germany 15.10.2015 - 17.10.2015

Spontaneous calcium elevations in microglia

L. Korvers, V. Matyash, M. Semtner, H. Kettenmann

10th FENS forum of Neuroscience Copenhagen, Denmark 02.07.16 - 06.07.16

Talks

The complexity of gene therapy in nerve repair

L. Korvers

Hacking Health Berlin, Germany 12.03.2016

Spontaneous Ca^{2+} elevations in microglia

L. Korvers

MDC/FMP PhD retreat Joachimsthal, Germany 22.03.2016 - 24.03.2016

6 Acknowledgements

I would like to acknowledge professor Helmut Kettenmann for the opportunity to perform my doctoral research in his laboratory. Doctor Marcus Semtner and doctor Vitali Matyash for supervising the project and their technical input in Ca^{2+} imaging and programming with Igor Pro. Martin Mersch for isolating and imaging hGAMs, Amanda Costa for isolating mGAMs, the technicians Irene Haupt, Hanna Schmidt, Regina Piske and Maren Wendt for preparing the primary cultured microglia and Niklas Meyer for correcting the German abstract. I would like to thank doctor René Jüttner, who provided aliquots of caffeine, dantrolene and ryanodine to investigate IP_3R and RyR. The work was funded by the Deutscher Akademische Austauschdienst (DAAD) and supported by SFB TRR43 and NeuroCure.